New Jersey Institute of Technology
Digital Commons @ NJIT

Theses | Electronic Theses and Dissertations

Spring 5-31-1986

Measurements of basic semiconductor properties

Abdolreza Ariantaj
New Jersey Institute of Technology

Follow this and additional works at: https://digitalcommons.njit.edu/theses

Part of the Electrical and Electronics Commons

Recommended Citation

Ariantaj, Abdolreza, "Measurements of basic semiconductor properties" (1986). *Theses*. 1436.
https://digitalcommons.njit.edu/theses/1436

This Thesis is brought to you for free and open access by the Electronic Theses and Dissertations at Digital Commons @ NJIT. It has been accepted for inclusion in Theses by an authorized administrator of Digital Commons @ NJIT. For more information, please contact digitalcommons@njit.edu.

Copyright Warning & Restrictions

The copyright law of the United States (Title 17, United States Code) governs the making of photocopies or other reproductions of copyrighted material.

Under certain conditions specified in the law, libraries and archives are authorized to furnish a photocopy or other reproduction. One of these specified conditions is that the photocopy or reproduction is not to be "used for any purpose other than private study, scholarship, or research." If a, user makes a request for, or later uses, a photocopy or reproduction for purposes in excess of "fair use" that user may be liable for copyright infringement,

This institution reserves the right to refuse to accept a copying order if, in its judgment, fulfillment of the order would involve violation of copyright law.

Please Note: The author retains the copyright while the New Jersey Institute of Technology reserves the right to distribute this thesis or dissertation

Printing note: If you do not wish to print this page, then select "Pages from: first page # to: last page #" on the print dialog screen

NJIT
New Jersey's Science & Technology University

The Van Houten library has removed some of the personal information and all signatures from the approval page and biographical sketches of theses and dissertations in order to protect the identity of NJIT graduates and faculty.

ABSTRACT

Title of Thesis : Measurements of Basic Semiconductor Properties

Abdolreza Ariantaj , Master of Science , 1986

Thesis directed by : Professor Roy H. Cornely

Mobility, resistivity, and total impurity concentration of several purchased p-type silicon samples with known resistivities were measured by Hall effect experiments utilizing the Van Der Pauw method. The silicon samples will serve as Hall effect standards for future measurements on other semiconductor materials, particularly gallium nitride ion cluster beam (ICB) deposited thin films. The samples which were freshly etched with hydroflouric acid had measurement values of 455 $cm^2/V.sec$, 45.9 $\Omega.cm$, and 2.6 $\times 10^{14} cm^{-3}$ for mobility, resistivity, and total impurity concentration, respectively. The mobility values were within 9.9 per cent of the published values and the accuracy of the measurement was improved by modifying the current measurement device. Exposure time of more than 30 seconds between etching and aluminum contact deposition was found to cause errors of up to one order of magnitude in the mobility and carrier concentration measurements. X-ray diffraction

measurements [using the General Electric SPG 2 Spetrogoniometer and G.E. 700 Detector and chart recorder] with Copper Kα radiation, had an excellent degree of accuracy and precision and showed nearly identical intensity peak locations (within 99.94%) compared with the published data for $\langle 111 \rangle$ and $\langle 100 \rangle$ silicon and the gallium samples supplied by the ICB laboratory. A gallium thin film sample proved to be polycrystalline, composed of differently oriented tiny crystallites as observed by the numerous intensity peaks at various Bragg angles. This was accounted for by discovering that the gallium sample was evaporated onto the glass substrate rather than being deposited in the form of ion beam clusters as first expected.

MEASUREMENT OF BASIC SEMICONDUCTOR PROPERTIES

by

Abdolreza Ariantaj

Thesis submitted to the Faculty of the Graduate School of
the New Jersey Institute of Technology in partial fulfillment of
the requirements for the degree of
Master of Science in Electrical Engineering
1986

APPROVAL SHEET

Title of Thesis : Measurement of Basic Semiconductor Properties

Name of Candidate : Abdolreza Ariantaj
Master of Science , 1986

Thesis and Abstract Approved :

Dr. Roy H. Cornely Date
Professor
Department of Electrical Engineering

Signatures of other members of the thesis committee

_______________________ Date

_______________________ Date

_______________________ Date

VITA

Name : Abdolreza Ariantaj.

Permanent Address :

Degree and date to be conferred : M.S.E.E , 1986

Date of birth :

Place of birth :

Secondary Education : Town-Country High School , Austin, Texas , 1979.

Collegiate Institutions Attended	Dates	Degree	Date of Degree
Texas Tech University	9/79 to 8/84	B.S.E.E.	Oct. 1984
New Jersey Institute of Technology	9/84 to 5/86	M.S.E.E.	May 1986

Major : Electrical Engineering

Position Held : Research assistant , Drexler Microelectronics Laboratory,

New Jersey Institute of Technology , Newark , NJ.

Dedicated

to

my parents

ACKNOWLEDGMENTS

I am indebted to many people for their guidance and advice about this research. I would like to offer my inadequate acknowledgement of appreciation to Dr. Roy H. Cornely whom without this research would have been impossible. Dr. Lawrence Suchow of the Physics Department provided important contributions relating to the X-ray diffraction theory and techniques. I would like to thank my fellow graduate and undergraduate students who assisted me throughout my work. Finally, I would like to express my gratitude to my family who believed in me and gave me encouragement and support to achieve my greatest goal of all.

TABLE OF CONTENTS

CHAPTER	Page
I . INTRODUCTION	1
II . HALL EFFECT EXPERIMENTS	3
A. Theory and background	3
1. The Van Der Pauw method	6
B. Experimental measurements	11
1. Sample description	11
2. Equipment description	12
3. Measurement procedure	14
4. Results of the measurements	15
C. Calculated expected measurement values using published data	16
D. Discussion of the results and conclusion	20
III . X-RAY DIFFRACTION EXPERIMENTS	30
A. Theory and background	30
1. X-ray conceptual theory	30
a. Crystallography and the Bragg law	30
B. Experimental measurements	35
1. Description of samples	35

2. Description of the equipment 36

3. Measurement procedure 37

C. Calculations 38

D. Discussion of the results and conclusion 44

APPENDIX A. PROPERTIES OF SILICON AND GALLIUM 49

1. Properties of silicon 49

a. Silicon "d" spacings for different orientations 49

b. Chemical and molecular properties of silicon 50

2. Gallium intensity peaks 50

APPENDIX B. QUADRATIC FORMS OF MILLER INDICES 53

APPENDIX C. X-RAY DIFFRACTOMETER 56

1. Operation 56

a. Turn on procedure 56

b. Turn off procedure 58

2. Suggestions for improvements in X-ray measurements 59

a. JFET (NTE132) Replacement 59

b. Further recommendations 60

APPENDIX D. ETCHING PROCEDURE FOR DE-OXIDIZATION OF
SILICON SAMPLES 62
APPENDIX E. JEOL VACUUM EVAPORATOR OPERATION 64
APPENDIX F. PROOF OF THE VAN DER PAUW'S EQUATIONS ... 68
APPENDIX G. HALL EFFECT MEASUREMENTS AND
CALCULATION PROCEDURE 73
1. Hall effect measurement procedure 73
a. Preparation procedure 73
b. Voltage measurements procedure
with constant magnetic field 74
c. Voltage measurements procedure
with varying magnetic field 76
d. Recommendations for the future measurements 76
2. Hall effect calculation procedure 77
a. The related equations 77
b. Hall effect program for the HP11-C calculator 79
BIBLIOGRAPHY 82

LIST OF TABLES

Table	Title	Page
2-1	Hall effect equipment	12
2-2	Comparison of measured and published data	20
2-3	Maximum amd minimum voltage readings	22
2-4	Error margins for the measured values	23
2-5	Hall effect measurements for silicon sample no. 1	25
2-6	Hall effect measurements for silicon sample no. 2	26
2-7	Hall effect measurements for silicon sample no. 3	27
2-8	Hall effect measurements for silicon sample no. 4	28
2-9	Hall effect measurements for silicon sample no. 5	29
3-1	Comparison of gallium intensity peaks	47
A-1	Diffraction data for silicon (published data)	49
A-2	Diffraction data for gallium (published data)	51
G-1	List of inputs and their corresponding registers	79

LIST OF FIGURES

Figure	Title	Page
2-1	Typical Hall effect set-up	3
2-2	A sample with contacts	6
2-3	Hall effect correction factor "f" vs. $R_{MN,OP}/R_{NO,PM}$	8
2-3	Sample with contacts on a line	9
2-5	Hall effect current control box	13
2-6	Resistivity vs. dopant concentration for silicon	17
2-7	Mobility vs. total impurity concentration for silicon	18
3-1	Reflection and diffration of rays	31
3-2	Basic setup for a diffraction experiment	32
3-3	Diffraction of monochromatic rays by a crystal	33
3-4	X-ray Spectrogoniometer measurements for ⟨111⟩ silicon sample no. 1	39
3-5	X-ray spectra for ⟨111⟩ silicon sample # 1 using lower gain settings	40
3-6	X-ray Spectrogoniometer measurements for ⟨100⟩ silicon sample no. 2	39
3-7	X-ray spectra for ⟨100⟩ silicon sample # 2 using higher gain settings	40
3-8	X-ray Spectrogoniometer measurements for vacuum deposited gallium thin film	46

LIST OF FIGURES

Figure	Title	Page
D-1	Etching procedure summary	63
E-1	JEOL vacuum evaporator	64
F-1	Infinite sample with a point M	68
F-2	Current applied to a sample with points on a line	69
F-3	Semi-infinite sample with half the current applied	69
F-4	A sample with four points on a line	70
G-1	Van Der Pauw's correction factor "f" vs. $R_{MN,OP}/R_{NO,PM}$	81

I. INTRODUCTION

Progress in semiconductor processing and manufacturing has been very rapid in the recent decade due to the ever increasing need of the perfect material for different industrial and commercial purposes. Recent advancements in silicon, germanium, and gallium arsenide processing techniques have led to a greater demand for investigation and determination methods of these seminconductors' structures and their properties.

There is an extensive research and work being done on growth of gallium nitride thin films using Ion Cluster Beam Deposition (ICBD) techniques in the Drexler Microelectronics labratories headed by Dr. Roy H. Cornely. This project will eventually reach testing and measurement stages when the samples are produced which in turn necessitates the need for having Hall effect and X-ray diffraction standards to assure compatibility between the produced samples and the theoretical characteristics.

Mobility, resistivity, majority carrier concentration, type (p or n), internal crystal structure, orientation, and type of the semiconductor are among the experimental results of the investigative methods and measurements done on the samples. Silicon is used as a preliminary sample and because of its predictable properties, its known crystal structure, and its handling expense, the systematic error estimation

of the available equipment would be optimal. This thesis provides the necessary information and standards for the future experimentations on the gallium nitride samples.

The chapters are organized in a sequence to provide gradual exposure and development of the experimentation methods and ideas. The appendices are included to accomodate the details and the operational procedures for the experiments used. Chapter two concerns Hall effect theory and the specific method used to measure mobility , resistivity, majority carrier concentration, and type (p or n), with mobility as the main property for the comparison. Chapter three discusses the X-ray diffraction experiments on different silicon samples and some gallium thin film samples, made by the Drexler Microelectronics Labratories of NJIT, and compares these results with the theoretical characteristics. There are many suggestions and recommendations given to modify and improve the equipments and their performance throughout this thesis. The modified operational procedures, given in the appendices, furnish the necessary information and guidance towards accomplishment of the best possible outcome.

II. HALL EFFECT EXPERIMENTS

A. Theory and background [1]

Hall Effect is a scientific procedure formulated by E. H. Hall which leads to derivation of many semiconductor properties such as : resistivity, type (p or n), majority carrier concentration, majority carrier mobility, Hall voltage, and the Hall coefficient.

If a magnetic field B is applied perpendicular to the direction of an applied current in a semiconductor it alters the current path.

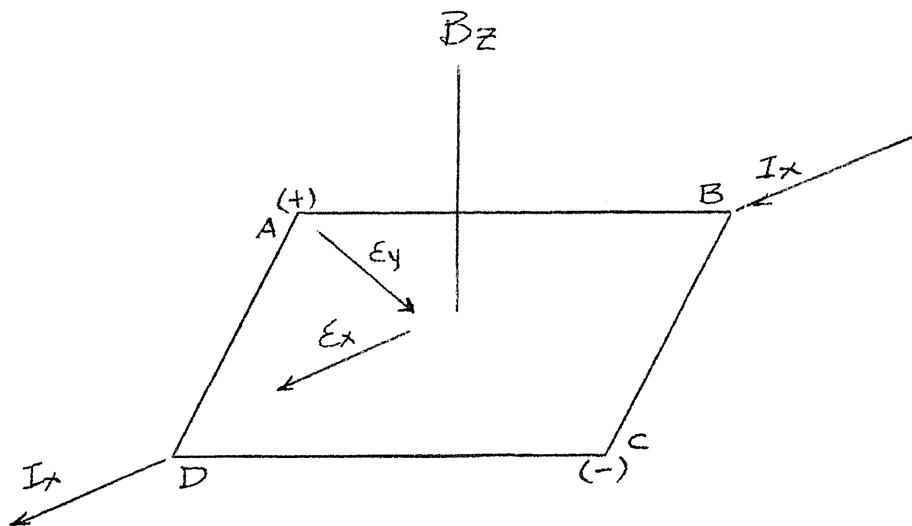

Figure 2-1 Typical Hall effect set-up

Each carrier, with an electronic charge q and a velocity of ν, experiences a force F caused by the magnetic field B and the electric field $\mathcal{E}$:

$$F = q.(\mathcal{E} \times \nu B) \qquad (2-1)$$

considering the y-component of this force we have:

$$F_y = q.(\mathcal{E}_y - \nu_x.B_z) \qquad (2-2)$$

If there is to be a zero net force on each carrier then the following equation must be satisfied :

$$\mathcal{E}_y = \nu_x.B_z \qquad (2-3)$$

where $\mathcal{E}_y$ is called the Hall effect and the Hall voltage is then:

$$V_{AB} = \mathcal{E}_y.w \qquad (2-4)$$

The current density J and the Hall effect are related by equations (2-5a) and (2-5b) for different types of materials: for p-type

$$J_x = q.p_o.v_x$$

or

$$I_x = q.p_o.v_x.l \qquad (2-5a)$$

for n-type

$$J_x = -q.n_o.v_x$$

or

$$I_x = -q.n_o.v_x.l \qquad (2-5b)$$

Where p_o and n_o are the majority carrier concentrations. Equations (2-3) and (2-5) yield: for p-type

$$\mathcal{E}_y = \frac{J_x B_z}{q p_o} = R_H J_x B_z \quad , \quad R_H = \frac{1}{q p_o} \qquad (2-6a)$$

and for n-type

$$\mathcal{E}_y = -\frac{J_x B_z}{q n_o} = R_H J_x B_z \quad , \quad R_H = -\frac{1}{q n_o} \qquad (2-6b)$$

Where R_H is the Hall Coefficient. Equations (2-5) and (2-6) lead to the derivation of equations (2-7): for p-type

$$p_o = \frac{1}{q R_H} = \frac{J_x B_z}{q \mathcal{E}_y} = \frac{I_x B_z w}{q t V_{AB}} \qquad (2-7a)$$

and for n-type

$$n_o = \frac{1}{q R_H} = \frac{J_x B_z}{q \mathcal{E}_y} = \frac{I_x B_z w}{q t V_{AB}} \qquad (2-7b)$$

So from these two above equations the values of the concentration for the majority carriers are found since the current I, the magnetic field B, the Hall voltage V_H, and the sample thickness are all measureable quantities.

The resistivity of a sample is given by equation (2-8):

$$\rho = \frac{Rwt}{l} = \frac{V_{cd} w t}{I_x l} \qquad (2-8)$$

Now the conductivity σ is the reciprocal of the resistivity, therefore the mobility of the majority carriers is the ratio of the Hall coefficient and the conductivity:

$$\mu_p = \frac{\sigma}{qp_o} = \frac{1/\rho}{1/R_H} = \frac{R_H}{\sigma}(p - type) \qquad (2-9a)$$

$$\mu_n = \frac{\sigma}{qn_o} = \frac{1/\rho}{1/R_H} = \frac{R_H}{\sigma}(n - type) \qquad (2-9b)$$

1. The Van Der Pauw method[2]

The Van Der Pauw method, which is used for the Hall effect measurements, is briefly described here.

Consider a flat sample with four contacts M, N, O, and P on the periphery (figure 2-2):

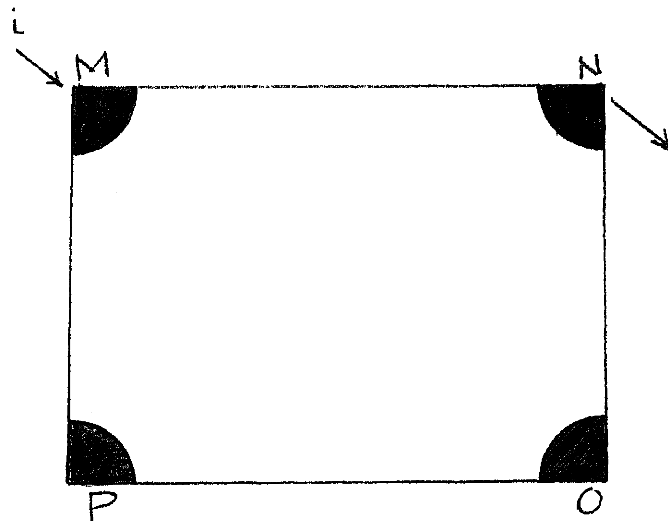

Figure 2-2 A sample with contacts

If a current i is applied to point M and taken off at point N, then the potential difference between points O and P is given by V_p - V_o and:

$$R_{MN,OP} = \frac{V_p - V_o}{i_{MN}}$$

and

$$R_{NO,PM} = \frac{V_m - V_p}{i_{NO}} \qquad (2-10)$$

Now $R_{MN,OP}$ and $R_{NO,PM}$ are related by (see appendix F):

$$\exp(\frac{-\pi d R_{MN,OP}}{\rho}) + \exp(\frac{-\pi d R_{NO,PM}}{\rho}) = 1 \qquad (2-11)$$

where d is the thickness of the sample and ρ is its resistivity.

If the sample is symmetric then:

$$R_{MN,OP} = R_{NO,PM} \qquad (2-12)$$

Therefore from the exponential (eq. 2-11) the resistivity is obtained:

$$\rho = \frac{\pi d R_{MN,OP}}{\ln 2} \qquad (2-13)$$

However, if the sample is not symmetric then ρ can be derived by:

$$\rho = \frac{\pi d f (R_{MN,OP} + R_{NO,PM})}{2 \ln 2} \qquad (2-14)$$

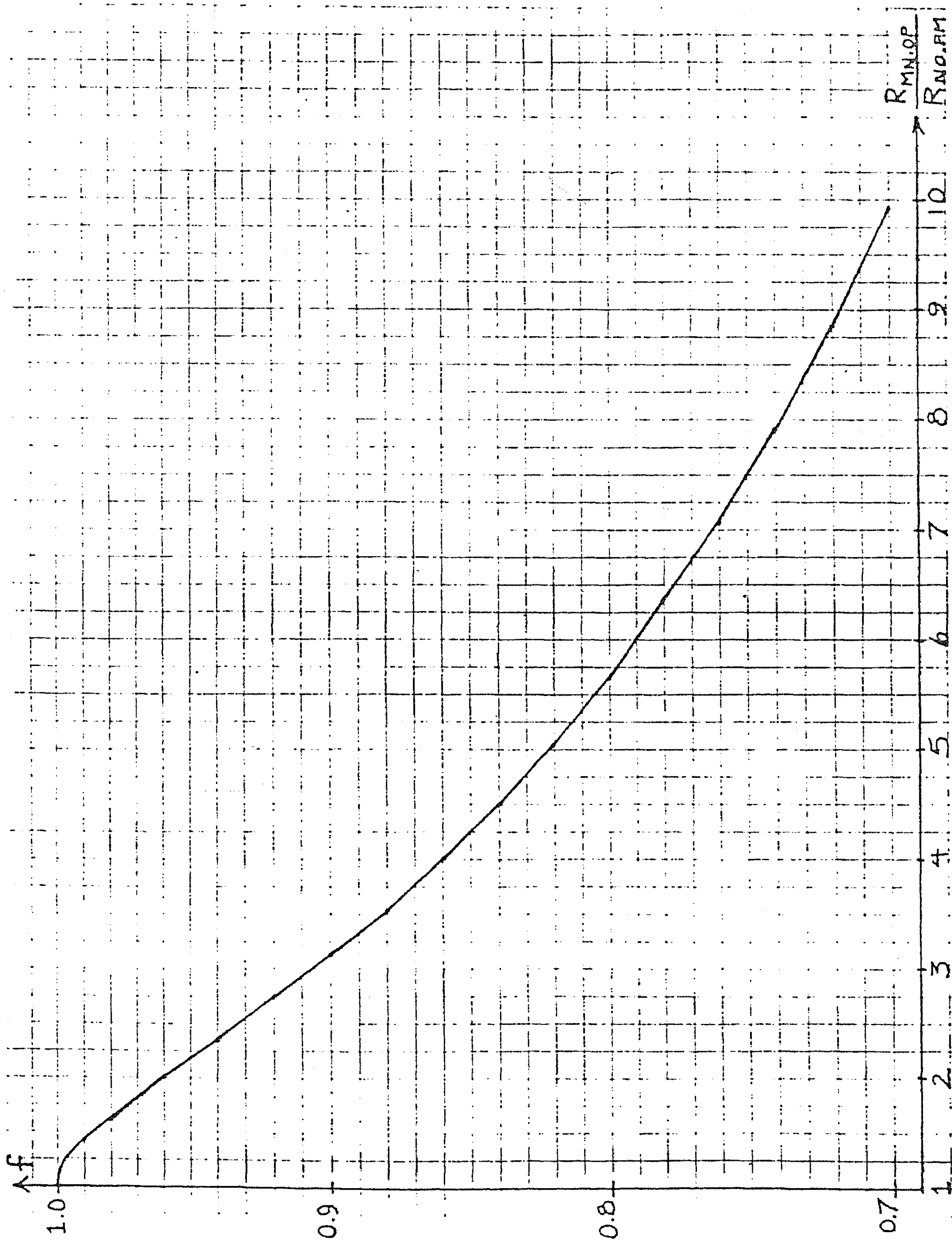

Figure 2-3 Hall effect correction factor "f" vs. $\frac{R_{MN,OP}}{R_{NO,PM}}$

Where f is the correction factor, which can be numerically derived from the figure 2-3. The function used to plot figure 2-3 is:

$$\cosh\left(\frac{(X-1)\ln 2}{(X+1)f}\right) = \frac{\exp(\ln 2/f)}{2} \qquad (2-15)$$

where X = $\frac{R_{MN,OP}}{R_{NO,PM}}$.

As mentioned earlier the proof of these equations is given in appendix F. For the Hall coefficient measurements we must have a sample with: 1) sufficiently small contacts, 2) contacts on the periphery, 3) uniform thickness, and 4) no physical holes in it.

If a current i is applied to a sample at point M and is taken off at point O we can measure (see figure 2-4) $R_{MO,NP}$:

$$R_{MO,NP} = \frac{V_P - V_N}{i_{MO}} \qquad (2-16)$$

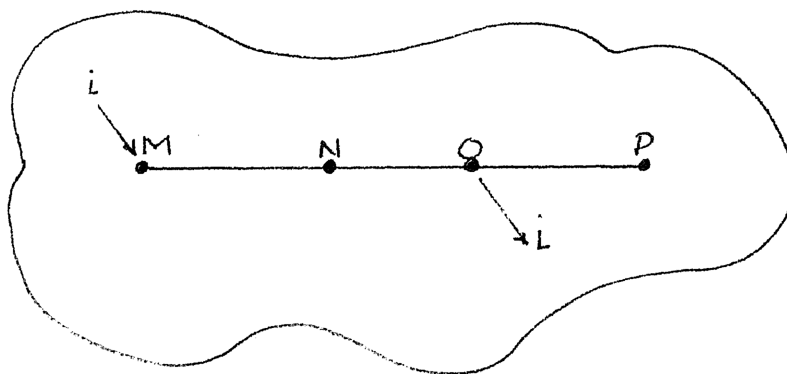

Figure 2-4 Sample with contacts on a line

If a magnetic field B is set up perpendicular to a sample with a thickness d, this would change the resistance given by equation (2-16) by an amount $\Delta R_{MO,NP}$. Then the Hall coefficient is given by:

$$R_H = \frac{d.\Delta R_{MO,NP}}{B} \qquad (2-17)$$

Under the magnetic induction B, the charge carriers with charge q, experience a force F which is:

$$F = q\nu B \qquad (2-18)$$

where ν is the velocity of the charge carriers. Another equation gives:

$$\nu = \frac{J}{qn_o} \qquad (2-19)$$

therefore

$$\mathcal{E}_H = \frac{JB}{qn_o} \qquad (2-20)$$

and

$$R_H = \frac{1}{qn_o} \qquad (2-21)$$

since q is known, n_o or p_o can be calculated from the above equations.

The magnetic field also causes a change in the potential difference. This potential difference change is given by equation (2-22).

$$\Delta(V_P - V_N) = \int_P^N \mathcal{E}_H.dS = R_H.B\int_P^N J.dS = R_H.B\frac{i_{MO}}{d} \qquad (2-22)$$

The theory for derivation of equation (2-22) is as follows: When a magnetic field is applied at right angle to the plane of the sample, there will be a change in the potential difference between points P and N. The transverse electric field $\mathcal{E}$ produced by the magnetic field is integrated along the path which runs from point P to point M. From equation (2-22) the Hall coefficient is derived and is given by equation (2-17).

In summary this method is used to measure the basic semiconductor properties of resistivity, mobility, Hall coefficient, and majority carrier concentration. To obtain the values for these properties several voltage and current measurements should be made with and without the presence of a magnetic field.

B. Experimental measurements

1. Description of the samples

The samples used were silicon squares of 1 cm sides cut from p-type boron doped 2 inch round wafers. Their thickness was 10 mils. or 0.0254 cm. Before any Hall effect measurements could be done on these samples, they had to be etched and then four aluminum contacts had to be evaporated onto their peripheries. The etching procedure, which is used to remove the oxide layer, is discussed in detail in appendix D. After each sample is etched it must be immediately (within 15 to 30 seconds) placed in the evaporator chamber to avoid further oxidization. The

samples should be square shaped and a side dimension of 1 cm is ideal for the Hall effect probes and the experiment.

After the samples were "dotted" with aluminum contacts (see appendix E for evaporation procedure and further details) they were ready for the Hall effect experiment.

2. Description of the equipment

Table 2-1 shows a list of the necessary equipment for the Hall effect set up and those that are already available or used in room 422 of the Tiernan building.

NO.	NECESSARY EQUIPMENT	AVAILABLE EQUIPMENT
1	Variable Magnetic Field Supply	water cooled VARIAN V2900 regulated magnet power supply
2	Constant current source	Electronic Measurements Programmable Regatron with current control box
3	Accurate voltmeter	Keithly 616 Digital Electrometer
4	Sample holder with probes	Handmade two-sided holder with four probes on each side
5	Hall Effect Box / Switch	Hall Effect Control Box
6	Vacuum Pump with pressure Indicator gauge	W.M. Welch Mfr. Co. Pump with Hastings Vacuum gauge
7	Curve Tracer	Tektronix type 575 Curve Tracer

TABLE 2-1 HALL EFFECT EQUIPMENT

The constant current source is a variable DC power supply connected to a current control box which is shown in figure 2-5.

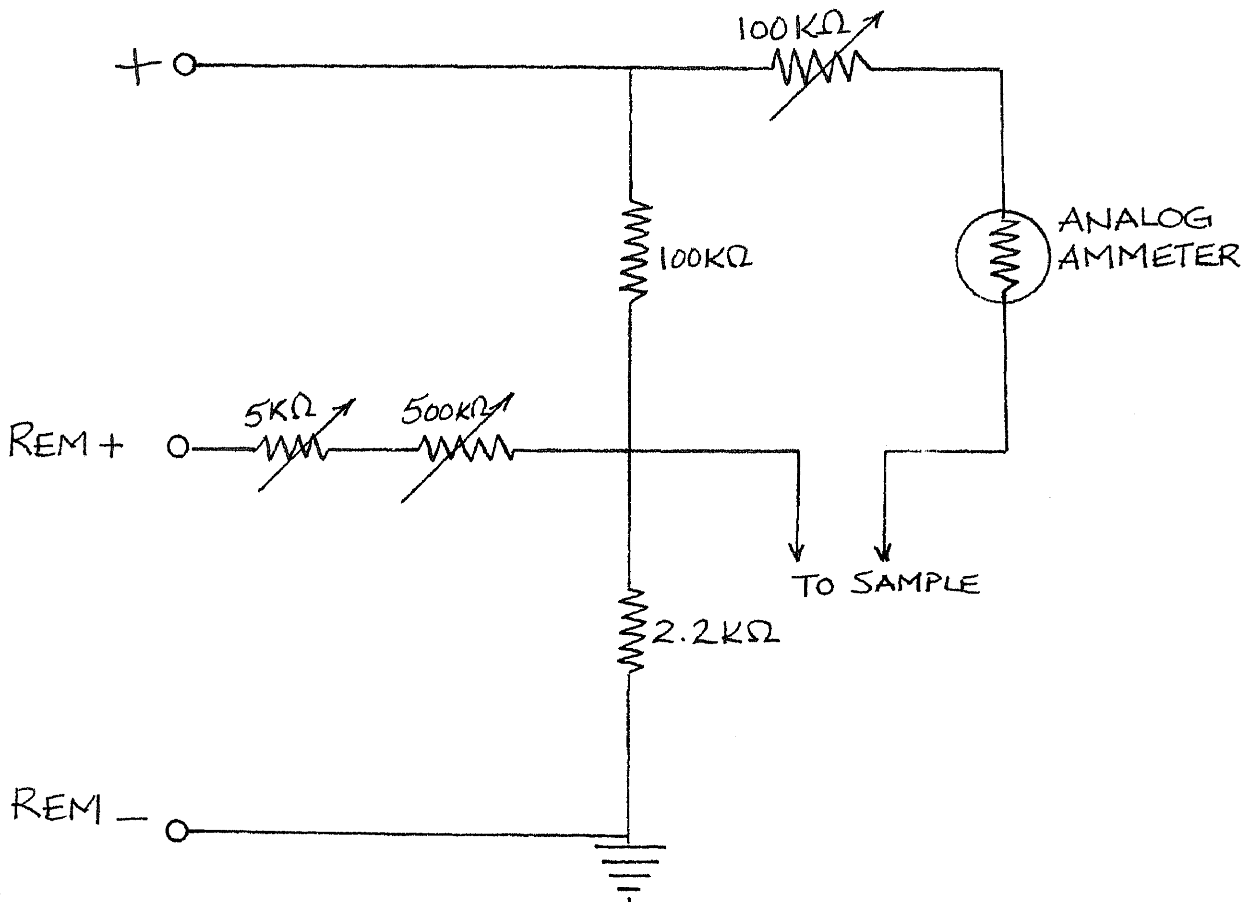

Figure 2-5 Hall effect current control box

This box was modified by placing a 500kΩ potentiometer in series with the REMOTE + terminal to enable more current to be pushed through in case of a highly resistive sample. Furthermore a 100KΩ potentiometer was placed in series with the

sample to further control the sample current. For further measurements with greater accuracy it is recommended that a 500Ω potentiometer be placed in series with the 500KΩ potentiometer (for purpose of fine tuning the current) and that the analog ammeter be replaced with a digital meter accurate up to 10 μA.

At the begining of this thesis work (Fall 1985) the Programmmable Regatron was malfunctioning and giving off-scale voltages and very high currents. Since this device has not been manufactured in 25 years, it had to be repaired by trying new tubes for the internal circuit. As a result two of the vacuum tubes (6L6 type) were replaced with new ones. The samples' contacts were tested and checked to avoid an open circuit path for the power supply which results in the off-scale voltages. There were also some problems with the sample holder. A few of the probe connections were loose. These connections were resoldered and tested for continuity and proved to be satisfactory.

3. Measurement procedure

Before any measurement is done, it is necessary to test that ohmic contacts exist between the silicon and the aluminum. A curve tracer can be used to assure an "ohmic contact" voltage to current relationship with very low resistance (typically less than 1kΩ for Si,Al contacts) characteristics. To test the sample on the curve tracer, place the sample in the sample holder and fasten the probe onto the sample making

sure of a contact which is not too tight. Then connect the leads from the sample holder to the collector and the emitter outlets on the curve tracer with the emitter grounded. Arrange the collector voltage and current settings to be low and observe the behavior of the contacts two at a time. If the sample has true ohmic contacts, measure the resistance from the slope at several different current levels. Otherwise, plot the general shape of the highly resistive sample to keep as a reference.

The basic approach of the Hall effect measurement is that a constant current (1.1 mA in this thesis work) is applied to two contacts of a sample at a time and a voltage is measured across the two other contacts. This is repeated in the presence of a magnetic field, normal to the sample, and then is repeated again with the magnetic field reversed. As mentioned before the resistivity, Hall voltage, mobility, majority carrier concentration, type (p or n), and the Hall coefficient are derived from the measured values of the magnetic field, applied current, and Hall voltages and use of equations (2-4) through (2-22). For a more detailed operational procedure of the Hall effect equipment and set-up, see appendix G.

4. Results of measurements

Twenty two samples of silicon were to be investigated from which ten turned out to be too large for the Hall effect sample holder, eight showed nonlinear current voltage characteristics with high resistive slopes, one showed inconsistent results, and

three showed satisfactory results (see tables 2-5 to 2-9 at the end of this chapter). The unsatisfactory results can be caused by the excessive surface oxidization that occurs between the etching and the evaporation of the samples. The measurements with a constant magnetic field of 3.5 kGauss were repeated eight times to assure accuracy, but because of lack of precision in the current control device results were far apart from each other. These readings were averaged and calculated to be :

1) $V_H = 34.1$ mV

2) $\mu_H = 454.9\ cm^2/V.sec$

3) p - type silicon

4) $p_o = 2.6 \times 10^{14} cm^{-3}$

5) $\rho = 47.3\ \Omega.cm$

6) $R_H = 22557\ cm^3/Coulomb$

C. Calculated expected measurement values using published data

The samples were all silicon with aluminum ohmic contacts, boron doped, p-type, with resistivities of 8 $\Omega.cm$ to 65 $\Omega.cm$. Figures 2-6 and 2-7 show plots of published resistivity and mobility versus total impurity concentration for p-type and n-type samples. These data are are presented for comparison with the experimental

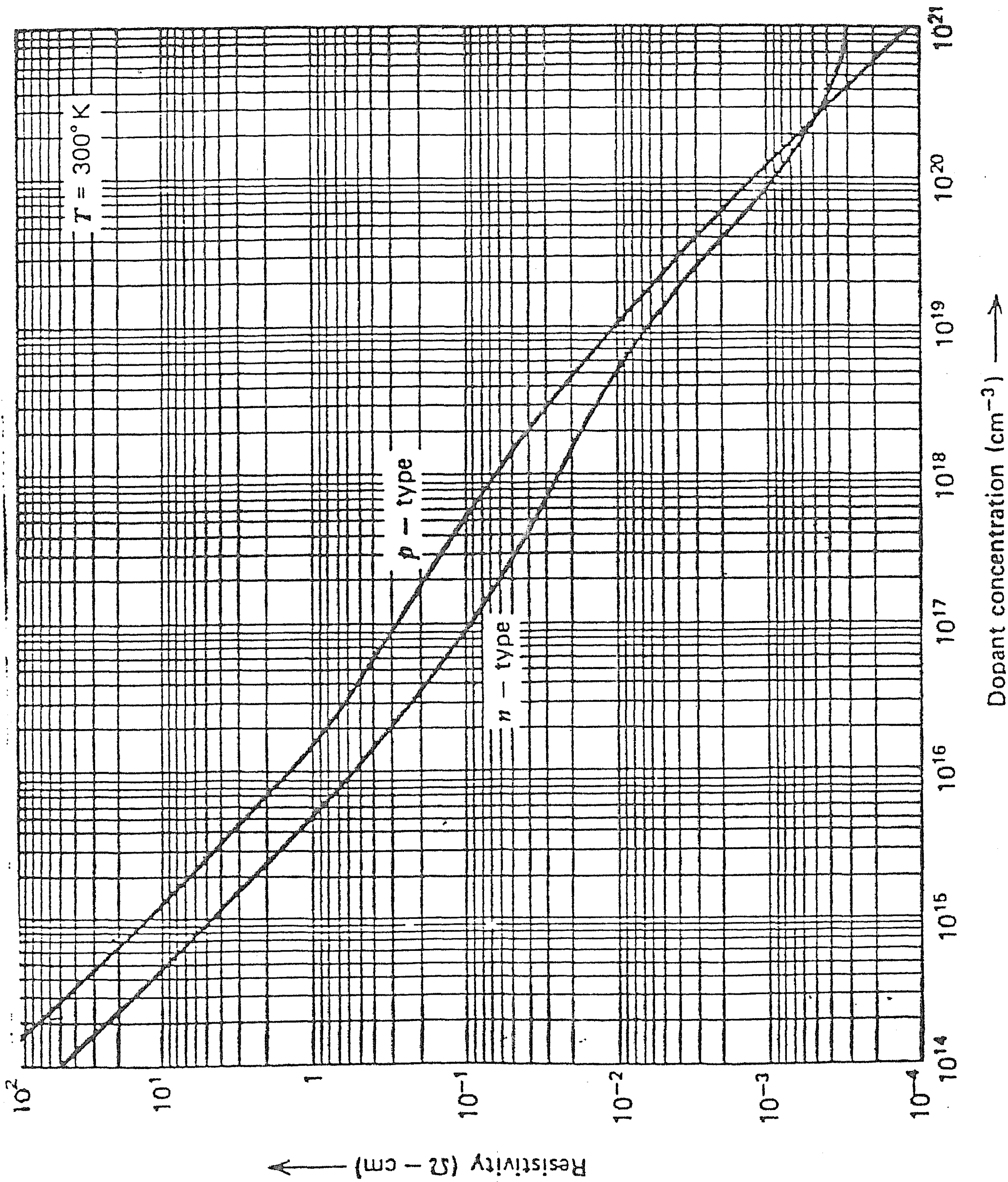

Figure 2-6 Resistivity vs. Dopant concentration;[3]
published data for silicon

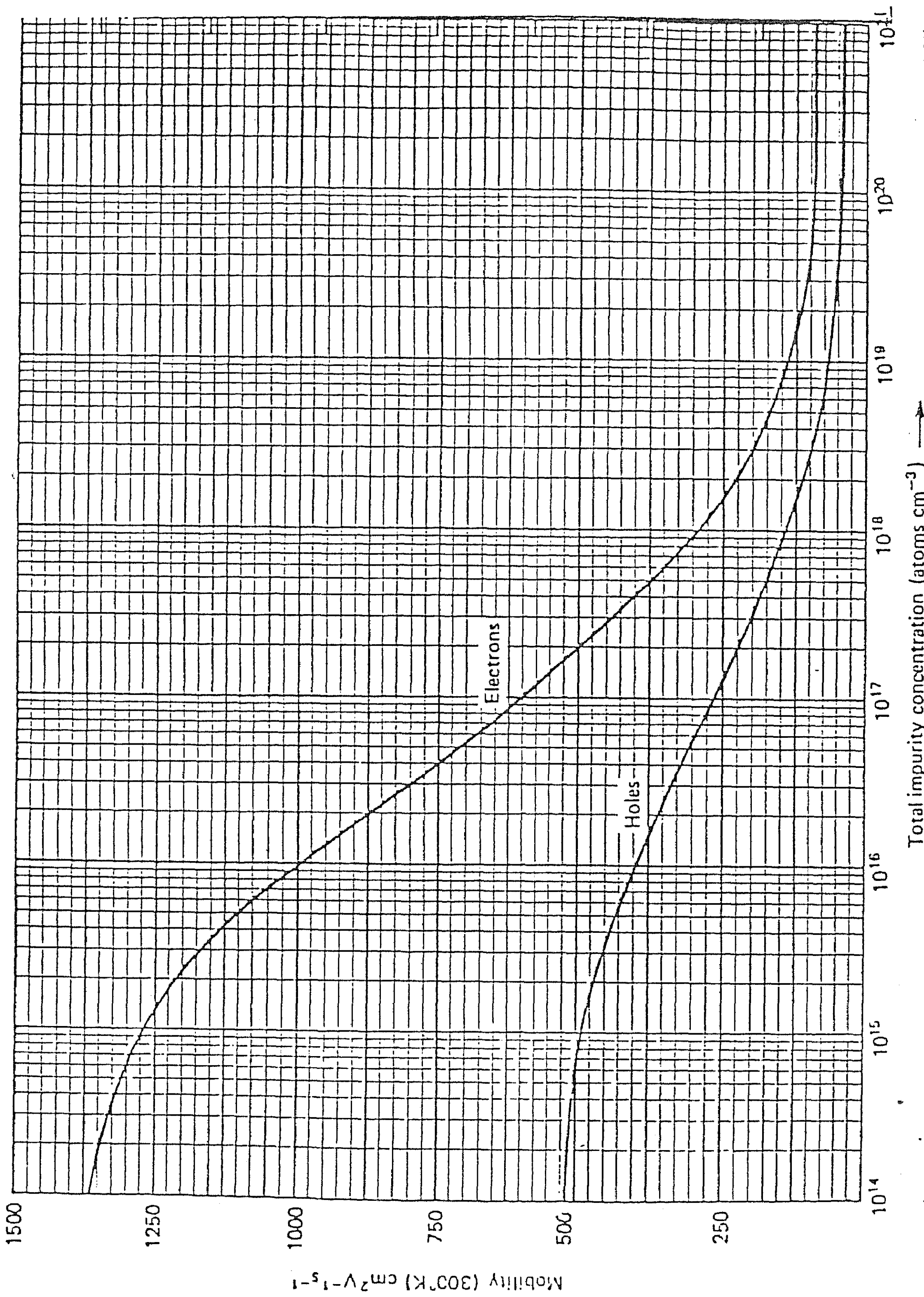

Figure 2-7 Mobility vs. total impurity concentration;[4] published data for silicon

results to verify the accuracy of the Hall effect measurements made and to confirm that the tested samples can be used as standards for future Hall effect measurement testing. From figure 2-6 it can be observed that for a silicon wafer with a resistivity of $45.9\Omega.cm$ the total impurity concentration that should be measured is approximately $2.9 \times 10^{14}\ cm^{-3}$ ($\pm 10^{13}$) and figure 2-7 shows that a mobility of approximately 505 $cm^2/V.sec$ should be measured for this sample. Equation (2-9) yields:

$$R_H = \rho.\mu_H = (45.9)(505) = 23180 cm^3/Coulomb \qquad (2-23)$$

From equation (2-7a), a Hall voltage of :

$$V_H = \frac{I_x B_z}{q p_o t} = \frac{R_H I_x B_z}{t} = 35.1 mV \qquad (2-24)$$

should be measured for these silicon samples, where I_x = 1.1 mA, R_H = 23180 $cm^3/Coulomb$, B_z = 3500 × 10^{-8} Weber/cm^2, and t = 0.0254 cm. Furthermore, p_o can also be calculated from equation (2-7a).

$$p_o = \frac{1}{qR_H} = \frac{I_x B_z w}{qtV_{AB}} = 2.7 \times 10^{14} cm^{-3} \qquad (2-25)$$

In sum the following are the calculated results of the Hall effect values expected to be measured using the purchased $45\Omega.cm \pm 50\%$ p-type silicon samples:

1) $R_H = 23180\ cm^3/Coulomb$

2) V_H = 35.1 mV

3) $p_o = 2.7 \times 10^{14}\ cm^{-3}$

and mobility for the p-type silicon was estimated from figure 2-7 to be $2.7 \times 10^{14} cm^2/V.sec$ assuming that the samples have the measured resistivity of $45.9\Omega.cm$. The value of $45\Omega.cm \pm$ 50% (appx. $25\Omega.cm$ to $65\Omega.cm$) was specified by the silicon vendor, Atomergic Chemetals Corporation.

D. Discussion of the results and conclusion

Table 2-2 shows the comparison between the measured values and the published data for silicon with the same resistivity as the tested samples and their difference (assuming that the published data are derived for the same type silicon samples with a single dopant concentration of boron.)

NO.	PARAMETER	MEASURED VALUES OF NJIT SAMPLES	VALUES FROM PUBLISHED DATA	% DIFFERENCE
1	V_H	34.1 mV	35.1 mV	2.85
2	μ_H	454.9 $cm^2/V.sec$	505 $cm^2/V.sec$	9.92
3	p_o	$2.6 \times 10^{14} cm^{-3}$	$2.7 \times 10^{14} cm^{-3}$	3.7
5	ρ	45.9 $\Omega.cm$	45.9 $\Omega.cm$	0
6	R_H	20363 cm^3/Coulomb	23180 cm^3/Coulomb	12.15

Table 2-2 Comparison of measured and published data

The per cent difference infers that the accuracy of the present Hall effect measuring equipment is 97.15% for V_H, 90.08% for μ_H, 96.3% for p_o, and 87.85%

for R_H. These results show that the NJIT measurements are nearly the same as the calculated data as far as Hall voltage and total impurity concentration are concerned. However,for the mobility and the Hall coefficient, there is a bigger difference. This difference was attributed to a lack of accuracy of the meters and sources used. The ammeter in the current control box is mainly the device that lacks accuracy. This analog meter is accurate only to 0.1 mA and can read values up to 3 mA. This inaccuracy and the possible current fluctuation can result in a larger variation of the measured voltages.

When the Keithly Digital Electrometer, which has an accuracy of $\pm 0.5\%$ and $1 \mu A$, was connected to the current control box to measure the sample current instead of the analog ammeter, it was observed that for a reading of 1.15 mA on the analog ammeter, the Keithly multimeter measured a current of 1.201 mA and also for an analog reading of 1.05 mA, the Keithly multimeter reading was 1.112 mA. Therefore, it was concluded that the current source meter was accurate only to 4.9% and that there was considerable error in the current supplied to the silicon samples. Since the current control device lacks accuracy, to find the error in the voltage measurement values, caused by this inaccuracy, two sets of voltage readings were taken : one set for a sample current of 1.1mA+0.05mA=1.15 mA, and one set for a current of 1.1mA-0.05mA=1.05mA The results are listed in table 2-3.

Voltages / Current	V_2	V_3	V_4	V_5	V_6	V_7	V_8	V_9
1.201 mA Maximum	**.437**	**.469**	**.526**	**.607**	**.489**	**.590**	**.590**	**.474**
1.112 mA Minimum	**.397**	**.427**	**.449**	**.540**	**.434**	**.529**	**.527**	**.427**
Error %	**9.6**	**9.4**	**15.8**	**11.7**	**11.9**	**11.0**	**11.8**	**10.4**

Table 2-3 Maximum and minimum voltage readings

The error is calculated using equation (2-26):

$$\%Error = \frac{(V_{max} - V_{min})}{(V_{max} + V_{min})/2} \times 100 \qquad (2-26)$$

Since the Hall voltage is the average of four voltage differences (see eq. 2-27) the errors could add up to a very high level.

$$V_H = \frac{|V_6 - V_4| + |V_7 - V_5| + |V_8 - V_5| + |V_9 - V_4|}{4} \qquad (2-27)$$

Assuming that each voltage measurement is approximately up to 90 per cent accurate, the worst case of Hall voltage measurement would have an error margin of 80%. This margin was found by using for example the maximum value for V_6 and the minimum value for V_4 and so on in equation 2-27. So for each Hall voltage measurement there is a marginal error of $\pm40\%$. Furthermore, the Hall voltage is used for other calculations such as the mobility, the Hall coefficient, and the carrier

concentration. Other calculations lead to other error margins, for example in equation (G-2) if the maximum values of V_2 and V_3 and the minimum value of I is used and then the minimum values of V_2 and V_3 and the maximum value of I is used then a marginal error of ± 14.3 is obtained. Similarly, equations G-3 through G-5 for ρ, R_H, and μ_H are used, utilizing the same maximum and minimum value substitution method to calculate the worst case error for each measured value. These calculated error margins for all of the Hall effect parameters are listed in table 2-4.

NO.	MEASURED PARAMETER	ERROR MARGIN %
1	V_H	**±44.5**
2	μ_H	**±41.1**
3	p_o	**±65.4**
4	ρ	**±14.3**
5	R_H	**±59.1**

Table 2-4 Error margins for the measured values

Since the error margin is so large in these measurements, it is recommended that the current control device and the ammeter be modified to the previously given specifications so that the current measurement would be accurate up to 0.5 percent instead of the present 5 percent accuracy. This would in turn lower the error margins for the other Hall effect parameters by one order of magnitude. Therefore, it is

recommended that the Drexler Laboratories purchased a current meter such as the Hewlett-Packard 3438A multimeter or its equivalent ($3\frac{1}{2}$ digit display, autoranging, and with minimum accuracy of .5%).

In conclusion, the Hall effect experiment components have undergone major repairs and modifications to produce these satisfactory results: The Programmable Regatron Power Supply 6L6 vacuum tubes were replaced; the current control device was modified to cover a wider range of sample currents; and the sample holder's probes were resoldered and tested. The three silicon samples which showed characteristics comparable to the published data can now be used as standards to assure that the Hall effect equipments are properly functioning. This method will be fully utilized when the gallium nitride samples, produced by the ICBD laboratory, reach testing stages. It will serve as a tool for measuring the properties of the future samples in order to eventually improve the processing and manufacturing techniques through comparison of the measured properties of produced samples under different processing conditions.

HALL EFFECT DATA SHEET

SAMPLE NO. : 1 T = ROOM TEMPERATURE

EXPERIMENTOR'S INITIALS : A.A. THICKNESS (IF KNOWN) : 0.0254 cm PROBE : 1

COMPLETE IF SAMPLE HAS BEEN ANNEALED

ANNEALING RUN: A_ Hg TEMP ______

SUBSTRATE TEMP. ________

Magnetic Field (Gauss)	MAGNET OFF				MAGNET ON @ NORM		MAGNET ON @ REV		V_H mV	u cm^2/V.Sec	P N	p_o cm^{-3}	R_H cm^3/col	ρ OHM$\cdot$cm
	2 & NORM	3 & NORM	1 & NORM	1 & REV	1 & NORM	1 & REV	1 & REV	1 & NORM						
3500	0.423	0.445	0.449	0.526	0.475	0.546	0.553	0.467	22.8	331	p	4.2E14	15050	45.4
3500	0.411	0.444	0.441	0.518	0.461	0.550	0.548	0.468	27.3	403	p	3.5E14	18027	44.7
3500	0.442	0.456	0.466	0.538	0.507	0.553	0.576	0.495	30.8	433	p	3.1E14	20342	47.0
3500	0.435	0.460	0.446	0.526	0.505	0.551	0.577	0.495	46.0	650	p	2.1E14	30431	46.8
3500	0.442	0.464	0.450	0.525	0.490	0.550	0.561	0.481	33.0	460	p	2.9E14	21831	47.4
3500	0.418	0.455	0.457	0.528	0.489	0.550	0.550	0.473	23.0	333	p	4.1E14	15215	45.7
3500	0.418	0.452	0.449	0.524	0.476	0.558	0.552	0.476	29.0	421	p	3.3E14	19185	45.5
3500	0.413	0.444	0.440	0.517	0.468	0.551	0.549	0.484	34.5	509	p	2.7E14	22823	44.8

MEASUREMENTS WITH VARIABLE MAGNETIC FIELDS

Magnetic Field (Gauss)	2 & NORM	3 & NORM	1 & NORM	1 & REV	1 & NORM	1 & REV	1 & REV	1 & NORM	V_H mV	u cm^2/V.Sec	P N	p_o cm^{-3}	R_H cm^3/col	ρ OHM$\cdot$cm
4620	0.434	0.448	0.471	0.535	0.508	0.574	0.568	0.471	38.8	414.2	P	3.2E14	19420	46.9
4340	0.416	0.472	0.440	0.543	0.488	0.571	0.578	0.470	35.3	408.8	P	3.3E14	18806	46.0
2000	0.410	0.470	0.454	0.541	0.467	0.560	0.562	0.464	15.8	400.0	P	3.4E14	18234	45.6
1000	0.412	0.472	0.452	0.544	0.458	0.536	0.551	0.462	7.8	391.8	P	3.5E14	17944	45.8
765	0.404	0.469	0.454	0.540	0.461	0.547	0.545	0.456	5.3	351.4	P	3.9E14	15890	45.2
432	0.402	0.465	0.450	0.541	0.454	0.548	0.541	0.444	4.3	507.2	P	2.8E14	22779	44.9
250	0.405	0.467	0.452	0.541	0.454	0.548	0.546	0.452	3.5	710.4	P	1.9E14	32416	45.6
165	0.401	0.470	0.453	0.545	0.456	0.547	0.546	0.458	2.8	846.7	P	1.6E14	35590	45.6

Table 2-5 Hall effect measurements for Silicon sample no. 1

HALL EFFECT DATA SHEET

SAMPLE NO. : 2 T = ROOM TEMPERATURE

EXPERIMENTOR'S INITIALS : A.A. THICKNESS (IF KNOWN) : 0.0254 cm PROBE : 1

COMPLETE IF SAMPLE HAS BEEN ANNEALED

ANNEALING RUN: A_ Hg TEMP ______
SUBSTRATE TEMP. ________

Magnetic Field (Gauss)	MAGNET OFF				MAGNET ON @ NORM		MAGNET ON @ REV		V_H mV	u_H cm^2/V.Sec	P/N	p_o cm^{-3}	R_H cm^3/col	ρ OHM·CM
	2 & NORM	3 & NORM	1 & NORM	1 & REV	1 & NORM	1 & REV	1 & REV	1 & NORM						
3500	0.404	0.421	0.419	0.369	0.451	0.406	0.408	0.439	32.0	490.4	P	3.0 E 14	21169	43.2
3500	0.405	0.424	0.416	0.370	0.449	0.404	0.407	0.442	32.5	495.6	P	2.9 E 14	21500	43.4
3500	0.402	0.425	0.419	0.368	0.448	0.405	0.406	0.440	31.3	477.7	P	3.0 E 14	20673	43.3
3500	0.406	0.417	0.414	0.369	0.447	0.405	0.405	0.438	32.3	495.4	P	2.9 E 14	21335	43.1
3500	0.403	0.425	0.415	0.366	0.445	0.407	0.406	0.441	34.3	522.9	P	2.8 E 14	22658	43.3
3500	0.405	0.422	0.420	0.370	0.452	0.404	0.409	0.441	31.0	473.9	P	3.1 E 14	20508	43.3
3500	0.406	0.426	0.417	0.368	0.454	0.407	0.409	0.450	37.5	569.8	P	2.5 E 14	24808	43.5
3500	0.403	0.423	0.418	0.367	0.453	0.406	0.408	0.445	33.0	503.7	P	2.9 E 14	21807	43.3
MEASUREMENTS WITH VARIABLE MAGNETIC FIELDS														
4620	0.404	0.421	0.419	0.369	0.440	0.409	0.410	0.450	33.3	368.0	P	3.8 E 14	16664	43.2
4340	0.408	0.427	0.419	0.370	0.435	0.402	0.415	0.454	32.0	390.7	P	3.7 E 14	17072	43.7
2000	0.403	0.422	0.419	0.370	0.431	0.408	0.408	0.451	30.0	804.5	P	1.8 E 14	34731	43.2
1000	0.403	0.422	0.419	0.368	0.425	0.398	0.391	0.433	18.3	978.8	P	1.5 E 14	42256	43.2
765	0.405	0.421	0.420	0.370	0.425	0.400	0.395	0.429	17.3	1208	P	1.2 E 14	52209	43.2
432	0.404	0.423	0.417	0.370	0.421	0.398	0.399	0.427	17.8	2198	P	6.6 E 13	95135	43.3
250	0.404	0.421	0.416	0.373	0.417	0.389	0.389	0.416	8.3	1770	P	8.2 E 13	76408	43.2
165	0.403	0.421	0.418	0.375	0.419	0.386	0.387	0.415	6.8	2197	P	6.6 E 13	94721	43.1

Table 2-6 Hall effect measurements for Silicon sample no. 2

HALL EFFECT DATA SHEET

SAMPLE NO. : 3 T = ROOM TEMPERATURE

EXPERIMENTOR'S INITIALS : A.A. THICKNESS (IF KNOWN) : 0.0254 cm PROBE : 1

COMPLETE IF SAMPLE HAS BEEN ANNEALED

ANNEALING RUN: A_ Hg TEMP ______
SUBSTRATE TEMP. ________

Magnetic Field (Gauss)	MAGNET OFF				MAGNET ON @ NORM		MAGNET ON @ REV		V_H mV	μ_H cm^2/V.Sec	P/N	p_o cm^{-3}	R_H cm^3/col	ρ OHM-cm
	2 & NORM	3 & NORM	1 & NORM	1 & REV	1 & NORM	1 & REV	1 & REV	1 & NORM						
3500	0.703	0.491	0.547	0.557	0.586	0.610	0.602	0.580	42.5	459.2	P	2.2 E 14	28116	61.2
3500	0.705	0.493	0.540	0.558	0.588	0.611	0.605	0.576	46.0	495.3	P	2.1 E 14	30431	61.4
3500	0.705	0.496	0.546	0.556	0.587	0.609	0.601	0.578	42.8	473.3	P	2.2 E 14	28281	59.7
3500	0.704	0.490	0.545	0.554	0.586	0.601	0.603	0.581	43.3	482.0	P	2.2 E 14	28612	59.4
3500	0.696	0.492	0.546	0.558	0.587	0.605	0.604	0.579	41.8	467.7	P	2.2 E 14	27619	59.1
3500	0.701	0.484	0.542	0.558	0.589	0.614	0.606	0.577	46.5	522.2	P	2.3 E 14	30672	58.9
3500	0.701	0.488	0.541	0.559	0.584	0.604	0.611	0.579	44.5	498.0	P	2.0 E 14	29439	59.1
3500	0.703	0.491	0.544	0.557	0.587	0.608	0.605	0.578	43.9	485.4	P	2.2 E 14	29037	59.8
MEASUREMENTS WITH VARIABLE MAGNETIC FIELDS														
4620	0.701	0.489	0.544	0.557	0.589	0.611	0.603	0.580	45.3	371.6	P	2.8 E 14	22678	61.0
4340	0.702	0.490	0.546	0.559	0.588	0.611	0.603	0.580	43.0	375.3	P	2.7 E 14	22941	61.1
2000	0.699	0.488	0.547	0.556	0.587	0.612	0.602	0.585	45.0	855.9	P	1.2 E 14	52096	60.9
4000	0.698	0.491	0.541	0.556	0.586	0.613	0.601	0.581	45.8	1737	P	5.9 E 13	105929	61.0
765	0.704	0.491	0.545	0.559	0.586	0.612	0.600	0.586	44.0	2173	P	4.7 E 13	133173	61.3
432	0.703	0.492	0.546	0.557	0.585	0.611	0.600	0.587	44.3	3870	P	2.6 E 13	237168	61.3
250	0.701	0.487	0.543	0.556	0.585	0.610	0.600	0.587	46.0	6993	P	1.5 E 13	426033	60.9
865	0.695	0.490	0.544	0.555	0.586	0.609	0.600	0.587	46.0	10622	P	9.7 E 12	645505	60.8

Table 2-7 Hall effect measurements for Silicon sample no. 3

BAD SAMPLE

UNSATISFACTORY RESULTS

HALL EFFECT DATA SHEET

SAMPLE NO. : 4 T = ROOM TEMPERATURE

EXPERIMENTOR'S INITIALS : A.A. THICKNESS (IF KNOWN) : 0.0254 cm PROBE : 1

COMPLETE IF SAMPLE HAS BEEN ANNEALED

ANNEALING RUN: A_ Hg TEMP ______
SUBSTRATE TEMP. ________

Magnetic Field (Gauss)	MAGNET OFF				MAGNET ON @ NORM		MAGNET ON @ REV		V_H mV	u_H cm^2/V.Sec	P/N	p_o cm^{-3}	R_H cm^3/col	ρ OHM cm
	2 & NORM	3 & NORM	1 & NORM	1 & REV	1 & NORM	1 & REV	1 & REV	1 & NORM						
3500	1.041	1.187	1.180	1.210	1.190	1.203	1.208	1.178	5.25	29.7	P	1.8 E 15	3466	116.6
3500	1.057	1.162	1.168	1.192	1.172	1.189	1.208	1.166	2.75	15.62	P	3.4 E 15	1814	116.1
3500	1.030	1.167	1.162	1.191	1.166	1.191	1.194	1.159	2.75	15.78	P	3.4 E 15	1814	115.0
3500	1.027	1.178	1.159	1.197	1.173	1.190	1.195	1.168	9.25	52.89	P	1.0 E 15	6103	115.4
3500	1.055	1.174	1.170	1.199	1.172	1.197	1.204	1.170	1.50	8.48	P	6.3 E 15	990	116.6
3500	1.055	1.172	1.172	1.201	1.179	1.192	1.206	1.170	5.75	32.55	P	1.7 E 15	3793	116.5
3500	1.068	1.177	1.160	1.197	1.164	1.196	1.201	1.168	4.25	23.87	P	2.2 E 15	2803	117.5
MEASUREMENTS WITH VARIABLE MAGNETIC FIELDS														
4620	1.015	1.170	1.159	1.193	1.165	1.188	1.201	1.157	5.25	23.06	P	2.4 E 15	2624	113.8
4340	1.016	1.163	1.157	1.186	1.164	1.172	1.189	1.157	6.0	28.0	P	2.0 E 15	3192	114.0
2000	1.050	1.159	1.167	1.192	1.169	1.178	1.192	1.166	4.25	42.45	P	1.3 E 15	4907	115.6
4000	1.007	1.160	1.159	1.184	1.165	1.183	1.185	1.158	1.50	45.86	P	1.2 E 15	5195	113.3
765	1.055	1.158	1.157	1.183	1.157	1.181	1.182	1.154	1.50	42.43	P	1.27E 15	4913	115.8
432	1.011	1.154	1.160	1.187	1.163	1.187	1.187	1.163	1.50	79.49	P	7.8 E 14	8018	112.1
250	1.054	1.154	1.156	1.182	1.156	1.181	1.191	1.165	4.75	383.5	P	1.4 E 14	43872	114.4
865	1.016	1.159	1.153	1.187	1.173	1.195	1.195	1.171	13.5	1677	P	3.3 E 14	188923	112.7

Table 2-8 Hall effect measurements for Silicon sample no. 4

BAD SAMPLE

UNSATISFACTORY RESULT

HALL EFFECT DATA SHEET

SAMPLE NO. : 5 T = ROOM TEMPERATURE

EXPERIMENTOR'S INITIALS : A.A. THICKNESS (IF KNOWN) : 0.0254 cm PROBE : 1

COMPLETE IF SAMPLE HAS BEEN ANNEALED

ANNEALING RUN: A_ Hg TEMP _______
SUBSTRATE TEMP. _________

Magnetic Field (Gauss)	MAGNET OFF				MAGNET ON @ NORM		MAGNET ON @ REV		V_H mV	u 1/cm V.Sec	P/N	n cm^{-3}	R_H cm/col	OHM/cm
	2 & NORM	3 & NORM	1 & NORM	1 & REV	1 & NORM	1 & REV	1 & REV	1 & NORM						
3500	0.681	0.567	0.597	0.637	0.580	0.635	0.637	0.593	5.75	58.67	P	1.7 E 15	3793	64.7
3500	0.694	0.577	0.584	0.623	0.579	0.623	0.630	0.594	5.50	55.10	P	1.7 E 15	3629	65.8
3500	0.682	0.559	0.588	0.638	0.580	0.635	0.630	0.578	7.25	74.39	P	1.3 E 15	4783	64.3
3500	0.686	0.559	0.578	0.611	0.572	0.632	0.625	0.569	12.5	127.9	P	7.6 E 14	8247	64.5
3500	0.671	0.563	0.580	0.634	0.579	0.620	0.616	0.566	11.8	121.2	P	8.1 E 14	7752	63.9
3500	0.663	0.555	0.576	0.624	0.572	0.622	0.614	0.581	5.25	54.89	P	1.8 E 15	3464	63.1
3500	0.667	0.559	0.575	0.618	0.574	0.616	0.612	0.576	2.50	25.97	P	3.8 E 15	1649	63.5

MEASUREMENTS WITH VARIABLE MAGNETIC FIELDS

Magnetic Field (Gauss)	2 & NORM	3 & NORM	1 & NORM	1 & REV	1 & NORM	1 & REV	1 & REV	1 & NORM	V_H mV	u	P/N	n	R_H	OHM/cm
4620	0.727	0.583	0.612	0.653	0.605	0.655	0.650	0.607	4.25	31.14	P	2.9 E 15	2124	68.2
4340	0.714	0.590	0.616	0.653	0.611	0.650	0.671	0.638	12.0	94.04	P	1.0 E 15	6385	67.9
3000	0.780	0.589	0.614	0.659	0.611	0.632	0.656	0.610	9.25	150.6	P	5.9 E 14	10679	70.9
4000	0.711	0.583	0.614	0.647	0.594	0.639	0.642	0.599	13.0	445.5	P	2.1 E 14	30018	67.4
765	0.812	0.583	0.616	0.656	0.613	0.657	0.671	0.631	8.50	456.8	P	2.4 E 14	25656	71.9
432	0.710	0.586	0.619	0.660	0.616	0.660	0.662	0.616	2.01	158.4	P	5.9 E 14	10690	67.5
250	0.721	0.582	0.615	0.660	0.610	0.657	0.657	0.612	3.50	476.5	P	1.9 E 14	32327	67.8
865	0.705	0.584	0.611	0.657	0.607	0.654	0.656	0.605	3.50	729.8	P	1.3 E 14	48980	67.1

Table 2-9 Hall effect measurements for Silicon sample no. 5

III. X-RAY DIFFRACTION EXPERIMENTS

A. General theory and background [5]

X-Rays were discovered in 1895 by the German Physicist Roentgen and because of their unknown nature and characteristics the name X was given to these rays. These X-rays were later found to be useful in many experiments such as their diffraction when they are incident with an object.

1. X-ray conceptual theory [6]

X-ray diffraction methods are useful tools for experimentation of bulk semiconductors ,thin films, and metals. They give general microstructural information about the materials under investigation.

One method used to reveal the crystal structure of materials is the X-ray diffractometer method. A sample is placed in an intense X-ray beam which causes the elements of the sample to fluoresce, or give secondary X-rays, principally of the characteristic wavelength. This sample is then rotated through various angles while the beam reflected and diffracted by it is being measured in a fixed counter with a wide slit. The resulting graph of intensity versus the angle, which is recorded on a chart operated by the detector, is called a rocking curve.

a. Crystallography and the Bragg law [7]

The general idea for X-ray diffraction is shown in figure 3-1:

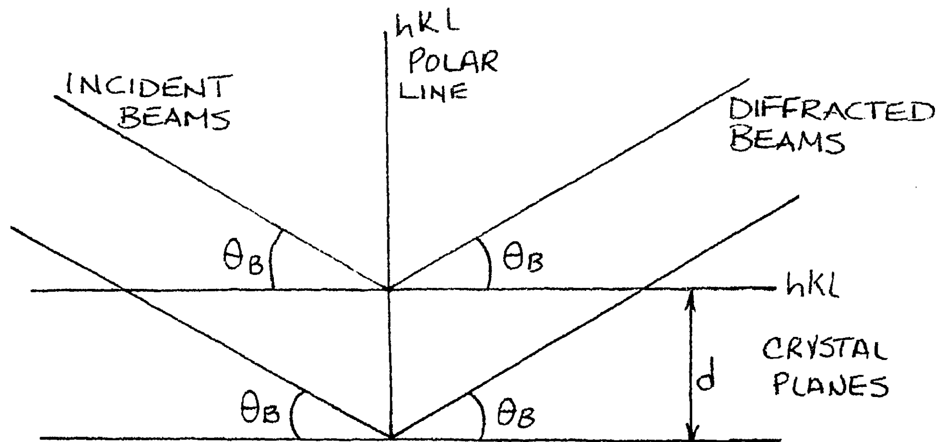

Figure 3-1 Reflection and diffraction of rays

As figure 3-1 indicates the hkl polar line is the line normal to the hkl plane of the crystal and the angle of incident equals the angle of diffraction. The Bragg angle θ_B is defined as the angle which the incident beam or the diffracted beam makes with the hkl plane of the crystal. The interplanar spacing of a crystal which is the distance between two parallel planes is found from the Bragg's law:

$$\lambda = 2d_{hkl}\sin\theta_B \qquad (3-1)$$

Where λ = wavelength of the diffracted radiation,

θ_B = The Bragg angle,and

d = Distance between the two parallel planes with Miller indices h,k,and l.

Since the wavelength of the radiation is known, the crystal dimensions and geometry can be determined from knowing diffraction patterns at several diffraction angles. The arrangements of atoms within the unit cell can only be determined from the intensity measurements of the radiation in each diffraction spot. This is then compared with the theoratically predicted density for several possible arrangements in the unit cell. Therefore the geometry of the lattice determines the geometry of the diffraction pattern and the distribution of atoms in a lattice determines the intensities of various diffraction spots. The basic set-up for the diffraction experiment is shown is figure 3-2:

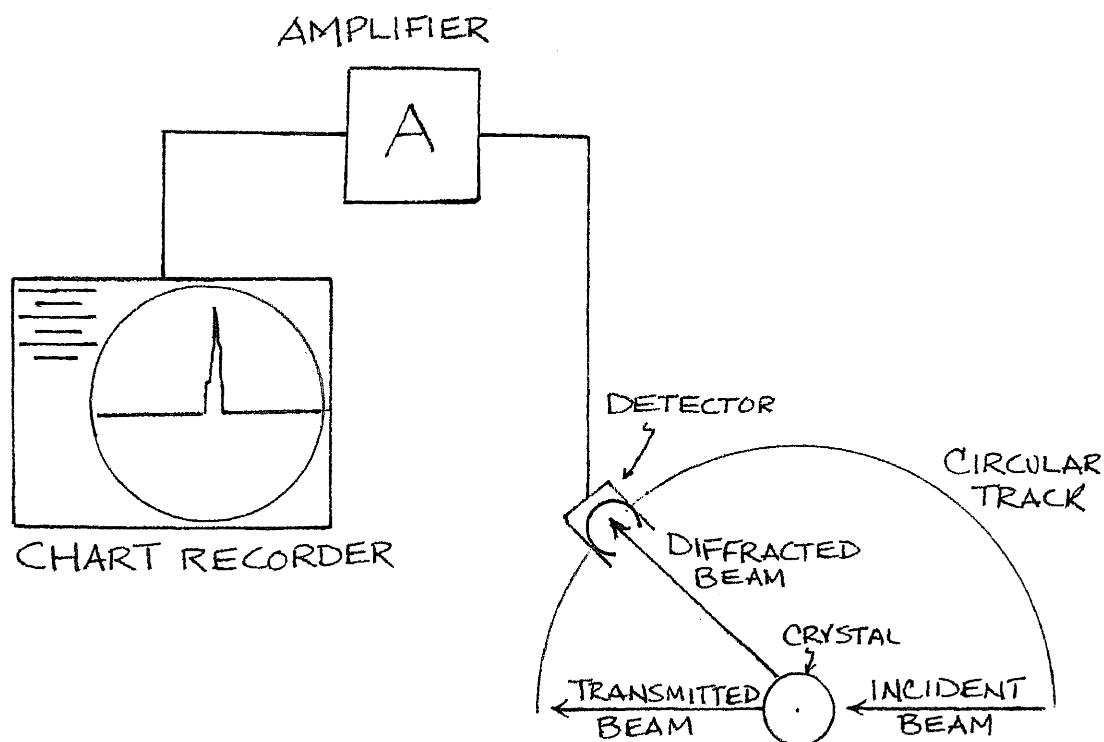

Figure 3-2 Basic set-up for a diffraction experiment

A sample is placed inside a circular rotating track within a high intensity X-ray. It is then rotated and the intensities are recorded for the different diffraction spots.

To get a clearer understanding of the resultant intensities that occur at different Bragg angles, the following theory is discussed. Consider a perfectly parallel monochromatic beam (of one frequency), of wavelength λ is incident on a crystal at an angle θ_B, called the Bragg angle, where θ_B is measured between the incident beam and the hkl crystal planes under consideration. Figure 3-3 describes the particular condition.

Figure 3-3 Diffraction of monochromatic rays by a crystal

Rays 1, 1a strike atoms K and P in the first plane and are scattered in all directions. However, they are in phase and reinforce each other in directions 1' , 1a' because of their path length. Also the rays scattered by all the atoms in the first plane in a parallel direction to each other are in phase and add their contributions to the diffracted beam. Now consider rays 1,2 which are scattered by atoms K and L. Scattered rays 1', 2' will be completly in phase if their path length is equal to a whole number of wavelengths or if:

$$n\lambda = 2d\sin\theta_B \qquad (3-2)$$

Equation (3-2) is the Bragg law equation and it was formulated by W.L. Bragg. It is essential to note that the diffracted beam from a crystal is made up of X-rays scattered by all the atoms of the crystal which lie in the path of the incident beam and also the diffraction of monochromatic X-rays takes place only at those particular angles of incidence which satisfy the Bragg law.

The spectra of an element is divided into two major radiation groups by wavelengths, these are:

1) K Radiation which in turn divides into $K\alpha_1$, $K\alpha_2$, $K\beta_1$.

2) L Radiation which consists of $L\alpha$,$L\beta_1$,$L\beta_2$.

There are other characteristic lines such as $L\gamma$, $L\eta$, $k\beta_2$ which are not of dominant intensity. Beacuse of their greater intensity, $K\alpha$ lines are used for analysis.

In conclusion, the incident X-ray beam is scattered by a large quantity of atoms. Because of the periodic arrangement of atoms in a lattice, the scattered X-rays have specific phase relations between them. Most phase relations cause destructive interference but in a very few scattering angles, due to in-phase diffracted rays, constructive interference is observed (e.g. a peak on the chart recorder).

B. Experimental measurements

1. Descriptions of samples

The samples under investigation were silicon wafers (samples 1 and 2) with $\langle 111 \rangle$ and $\langle 400 \rangle$ (same as $\langle 100 \rangle$) orientations. These samples were cut from 2 inch round wafers to fit the sample holder's maximum specifications which are:

1) Thickness = 3/8 in.

2) Width = 1 1/8 in.

3) Length = 3 in.

The polished sides of the samples were exposed to the X-rays for analysis. However, later it was found that this precaution was not a factor in the measurements but is recommended for greater accuracy.

In additions to the silicon samples, some gallium samples, supplied by the Ion Cluster Beam Laboratory, were tested. These samples were results of gallium deposition on clear slide glasses with evaporated aluminum side contacts. For the experiments the side with the gallium was exposed to the X-rays since the glass side tends to randomly scatter the X-rays due to its amorphous structure.

2. Description of the equipment

The Genaral Electric Spectrogoniometer, located in room B5 of the Faculty building of NJIT, was used to investigate crystal structures of the samples.

The sample is held in the sample holder in the sample chamber at a 30 degree angle from the horizon below the window of the X-ray tube. The fluorescent radiation, caused by the primary radiation striking the sample, emerging from the beam tunnel can be reflected by the flat analyzing crystal. This radiation is analyzed for characteristic wavelengths.[8]

As the spectrogoniometer manually turns through its 2θ range, it analyzes the X-ray spectra into wavelengths corresponding to the interplanar spacing "d"

of the flat crystal (see figure 3-2). The diffracted rays from the silicon sample are detected by a detector and then are amplified and recorded on the General Electric 700 detector, which prints out a graph of intensity versus the Bragg angle.

3. Measurement procedure

The basic procedure for finding the interplanar spacing of a crystal is as follows: 1) Find angle 2θ where the intensity peak is observed. 2) Find the line corresponding to this angle 2θ from the tables of interplanar spacing for angle 2θ - Direction 11710, published by the X-ray department of General Electric Corporation for Copper $K\alpha_1$ (Cu $K\alpha_1$) radiation. If this book is not available simply use the Bragg equation:

$$d = \frac{\lambda}{2\sin\theta_B} \qquad (3-3)$$

Where $\lambda = 1.5405$ Å for the Cu $K\alpha$ radiation and θ_B is determined from the location of the intensity peak.

When the interplanar spacing is found from the measurements, it must then be compared to the theoretical value for accuracy and precision considerations. The intensity peak amplitude and its area determine the structure and orientation of the samples; however, for silicon it can be found from an easier method which utilizes equation (3-4).[9]

$$d = \frac{a}{\sqrt{h^2 + k^2 + l^2}} \qquad (3-4)$$

Where d = interplanar spacing,

a = Lattice constant (for Si a=5.4309 Å),

h,k,l = Miller indices for determination of orientation

Since the samples used had orientations of $\langle 111 \rangle$ and $\langle 400 \rangle$ the quadratic sum of the Miller indices would be unique for each and can directly lead to the determination of these samples' orientations. A list of quadratic forms of Miller indices for different cubic structures of crystals is given in appendix B.

C. Calculations

Two types of silicon with different orientations were tested. The silicon samples with orientation $\langle 111 \rangle$ showed a major intensity peak at 28.4 degrees and a minor peak at 25.6 degrees. The lower peak is caused by the Copper $K\beta$ radiation (see figures 3-4 and 3-5).

For this Bragg angle of 28.4 the interplanar spacing is calculated from equation (3-3) to be:

$$d = \frac{\lambda}{2\sin\theta_B} = \frac{1.5405}{2\sin(28.4/2)} = 3.1399\mathring{A} \qquad (3-5)$$

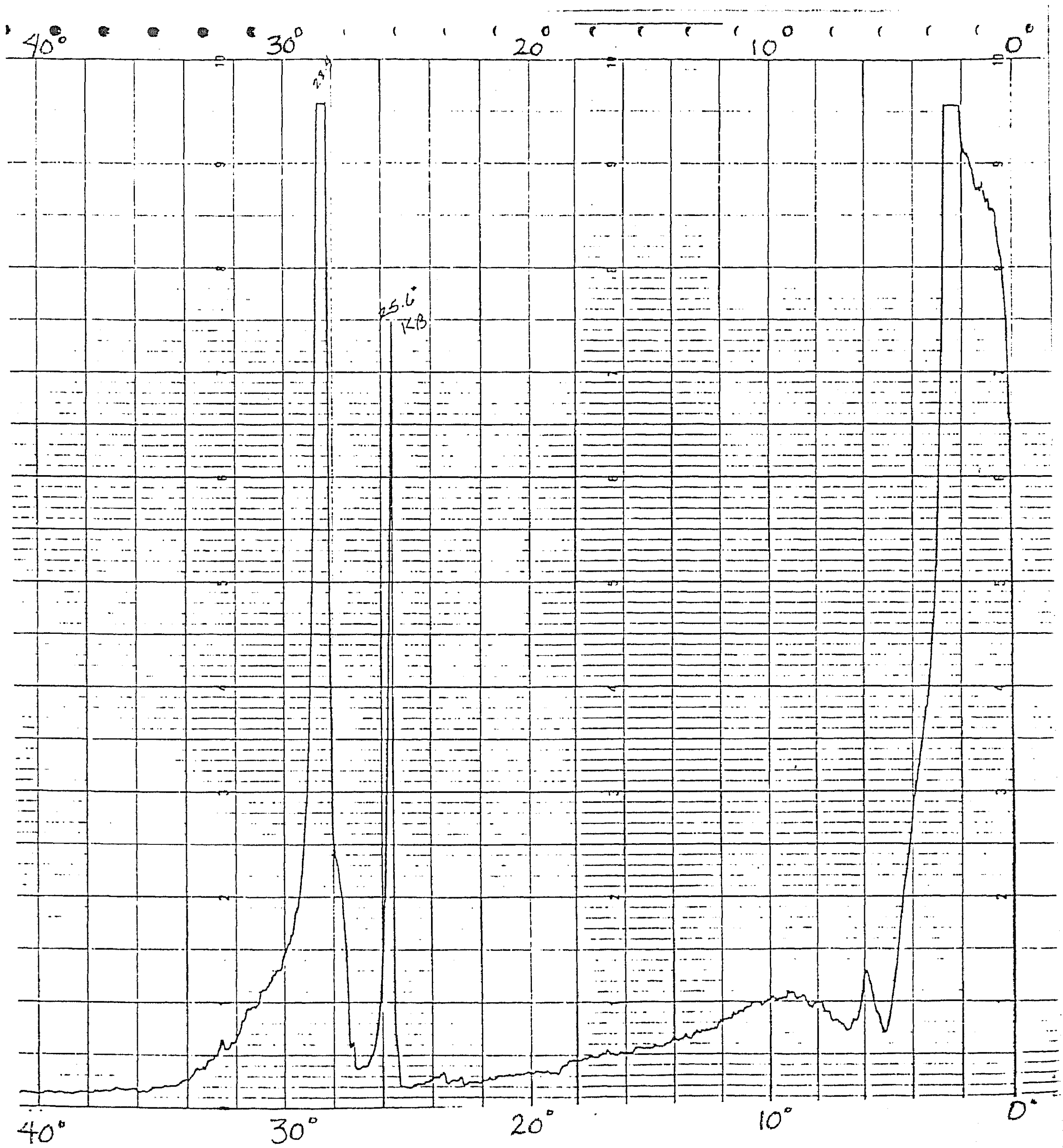

Figure 3-4 X-ray Spectrogoniometer measurements for silicon <111> no. 1

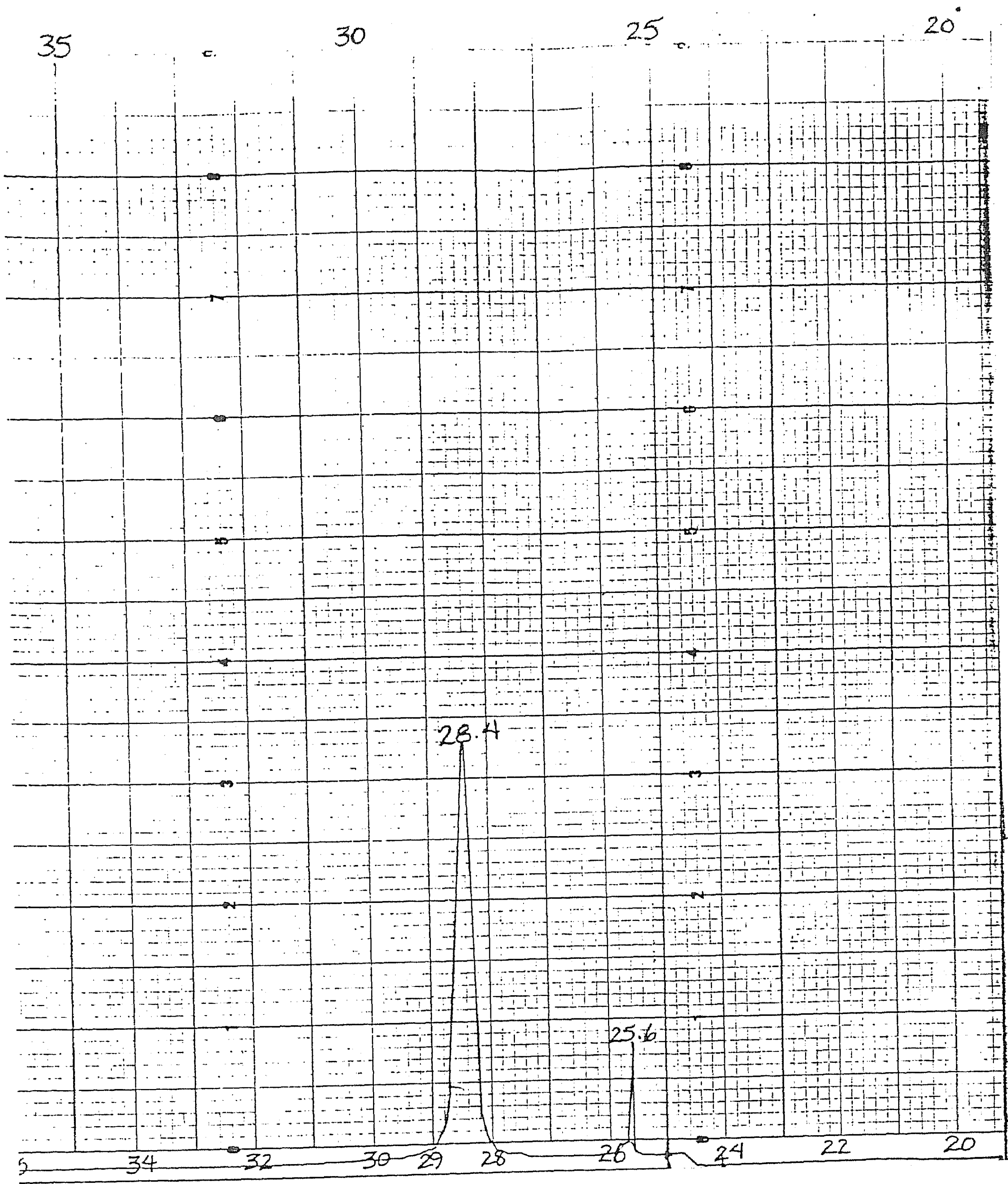

Figure 3-5 X-ray spectra for ⟨111⟩ silicon sample #1 using lower gain and slower scan settings

Now we can use equation (3-4) to get the quadratic sum of the Miller indices which helps to find the orientation of this sample.

$$h^2 + k^2 + l^2 = \left(\frac{a}{d}\right)^2 = \left(\frac{5.4309}{3.1399}\right)^2 = 2.9927 \qquad (3-6)$$

The closest whole number to this value is 3 which yields (see appendix B):

$$h = 1$$

$$k = 1 \qquad (3-7)$$

$$l = 1$$

Therefore the sample must have a surface orientation of $\langle 111 \rangle$.The $K\beta$ radiation can also be used to derive this information with a change of the wavelength value into equation (3-5).

For the second type of silicon the intensity peaks occured at 61.8 degrees and 69.2 degrees with the latter as the dominant ray which is the Cu $K\bar{\alpha}$ radiation (see figure 3-6). Figure 3-7 shows the X-ray spectra for the same silicon sample with higher gain settings. The two measured peaks are called the Kα doublets (Kα_1 and Kα_2), which can only be observed with the slowest spectrogoniometer speed and high sensitivity settings on the 700 Detector, since there are only a fraction of a degree apart from each other.

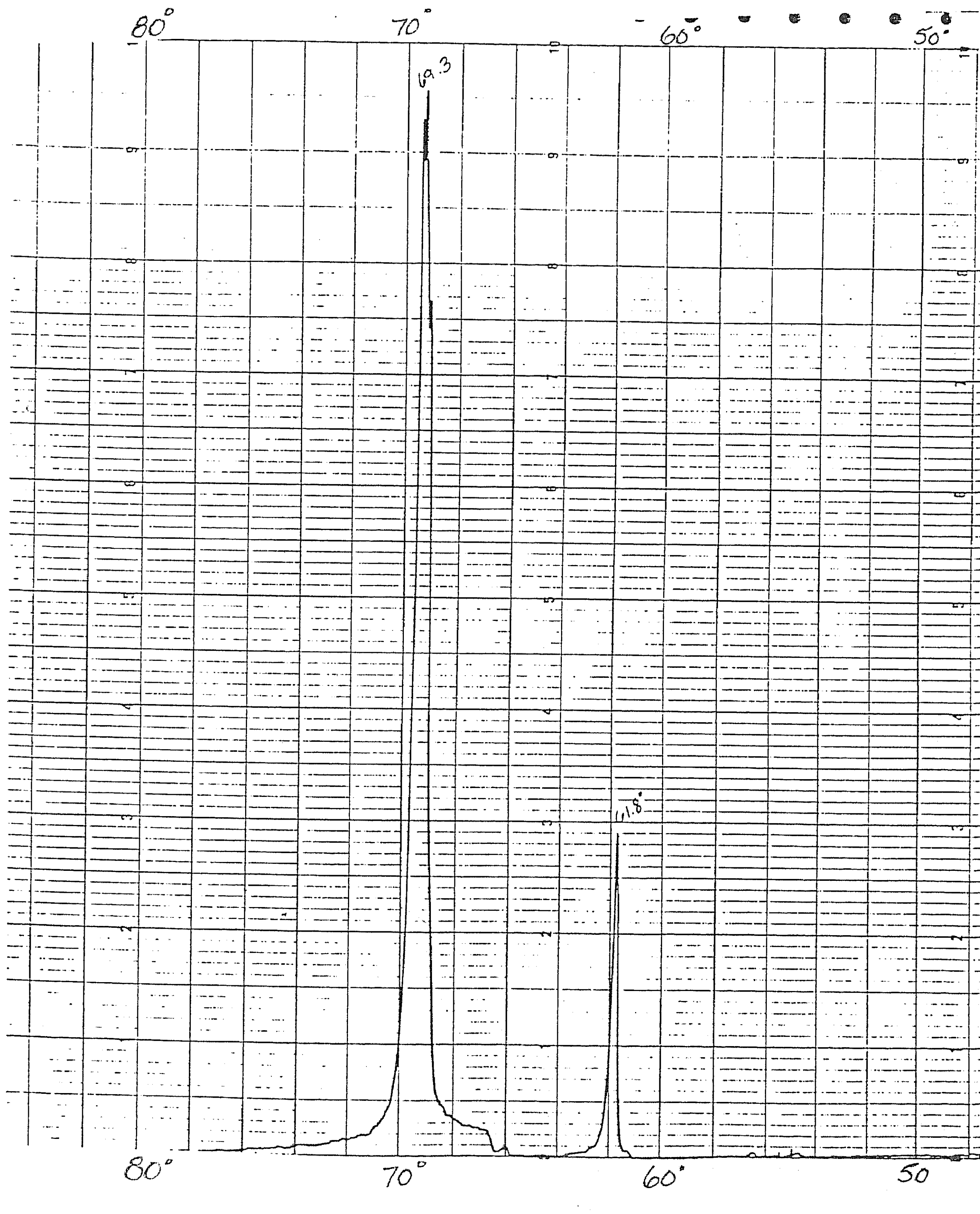

Figure 3-6 X-ray spectrogoniometer measurements for silicon ⟨100⟩ #2

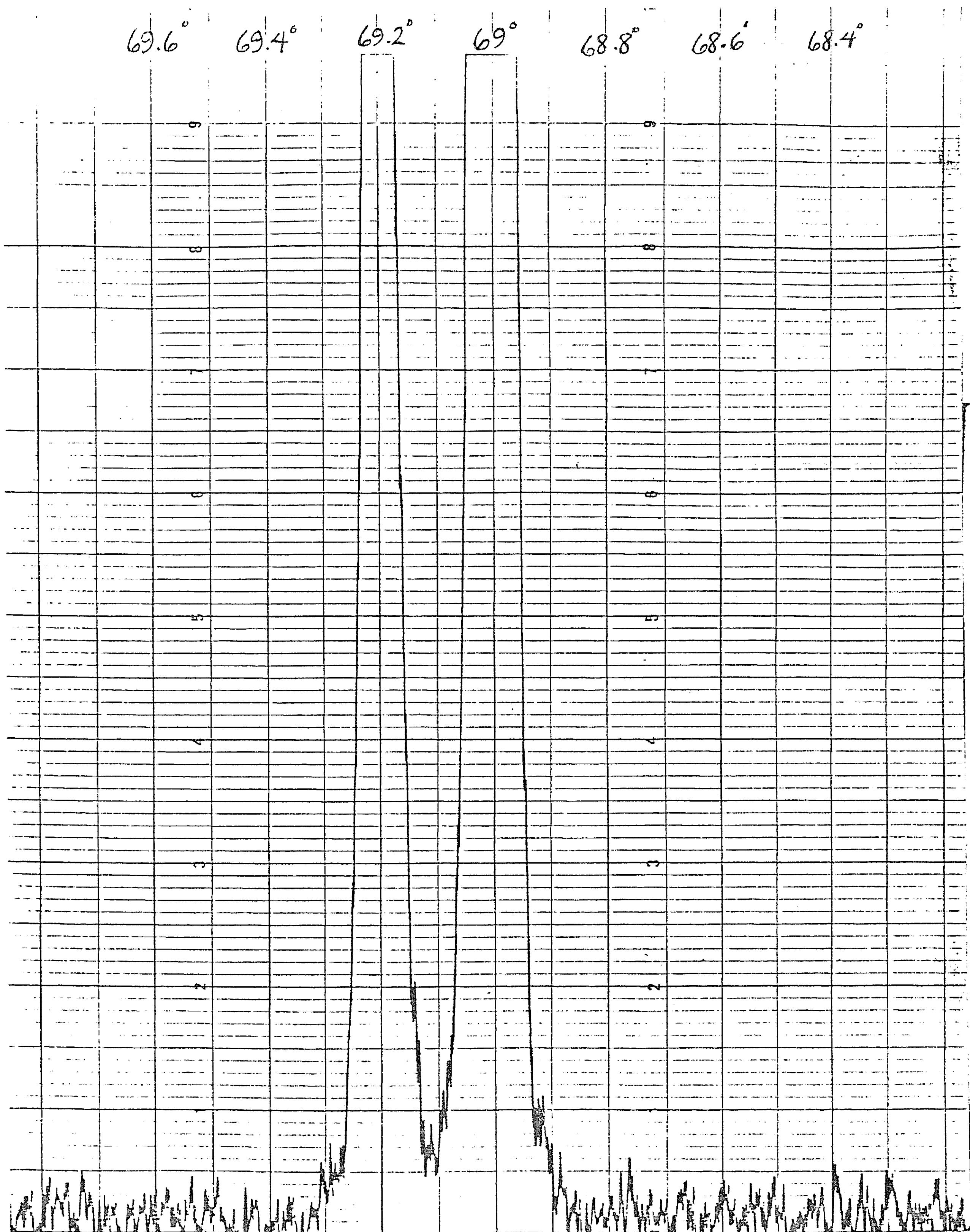

Figure 3-7 X-ray spectra for (100) silicon sample #2 using higher gain settings

Equation (3-3) yields:

$$d = \frac{\lambda}{2\sin\theta_B} = \frac{1.5405}{2\sin(69.2/2)} = 1.3564\mathring{A} \qquad (3-8)$$

This interplanar spacing is different from the previous sample's spacing because of the orientation difference. From equation (3-4) the quadratic sum of the Miller indices is found to be:

$$h^2 + k^2 + l^2 = \left(\frac{a}{d}\right)^2 = \left(\frac{5.4309}{1.3564}\right)^2 = 16.0313 \qquad (3-9)$$

Taking the closest whole number and consulting appendix B for the Miller indices under diamond cubic structures having values of 16, following results are obtained:

$$h = 4$$

$$k = 0 \qquad (3-10)$$

$$l = 0$$

So the silicon sample must have a $\langle 400 \rangle$ surface orientation which is the same as having an orientation of $\langle 100 \rangle$.

The gallium samples which were produced by the Ion Cluster Beam Deposition techniques were tested and the best result among those (sample no. 1) was taken to

be presented in this thesis as an additional standard (see figure 3-7). The results and a comparison between them and the theoretical values are given in the next section.

D. Discussion of the results and conclusion

For silicon samples with a $\langle 111 \rangle$ surface orientation of the theoretical interplanar spacing is 3.138 $\AA$ (see appendix A). This interplanar spacing was measured and calculated to be 3.1399 $\AA$, from the intensity peak at $2\theta_B = 28.4$ degrees. Therefore the accuracy of this measurement is:

$$\left(\frac{3.1380}{3.1399}\right) \times 100 = 99.94\% \qquad (3-11)$$

Furthermore the orientation of this sample was found to be $\langle 111 \rangle$, which is correct. The accuracy of the intensity peak measurements can be improved if the speed of the spectrogoniometer is decreased and the speed of the chart recorder is increased.

For the second set of silicon wafers with an orientation of $\langle 100 \rangle$, the predicted interplanar spacing is 1.357 $\AA$ (see appendix A). The measured value of the Si $\langle 100 \rangle$ "d" spacing was derived to be 1.3564 $\AA$. Therefore this measurement is accurate to:

$$\left(\frac{1.3464}{1.357}\right) \times 100 = 99.22\% \qquad (3-12)$$

Also the correct orientation was derived from appendix A to be $\langle 100 \rangle$, which is the same as an orientation of $\langle 400 \rangle$.

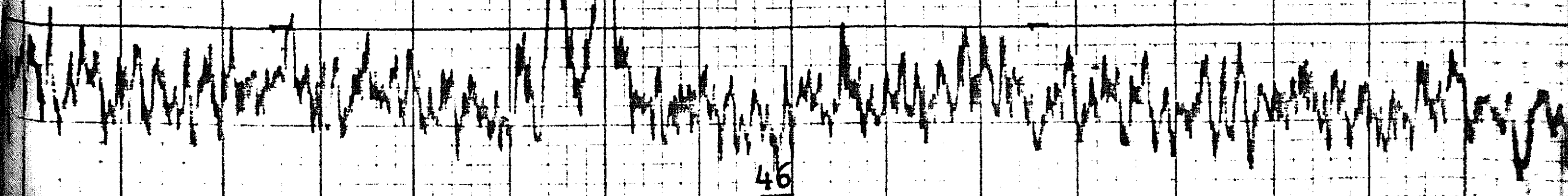

Figure 3-8 X-ray Spectrogoniometer measurements for vacuum deposited gallium thin film

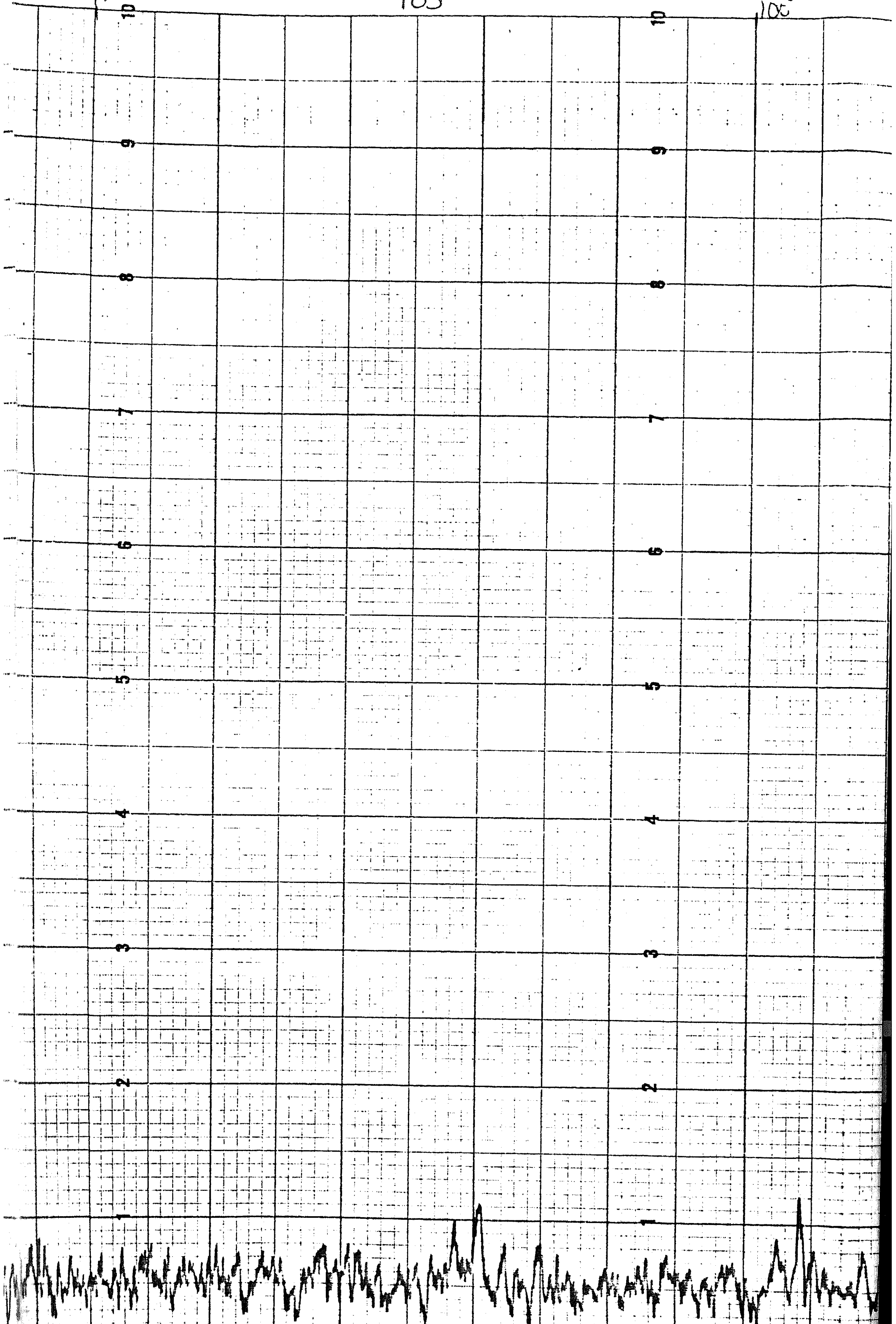
110°
105°
100°

95°   90°   85°

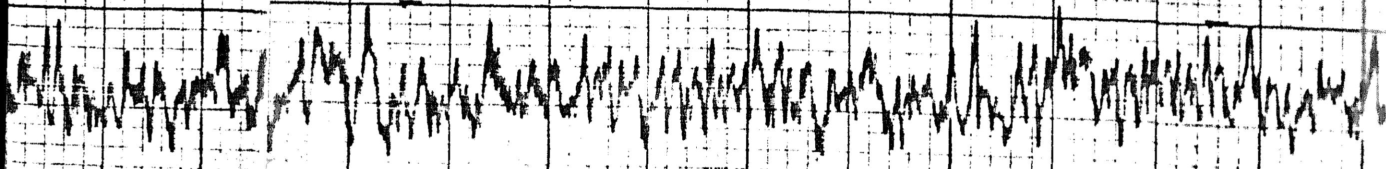

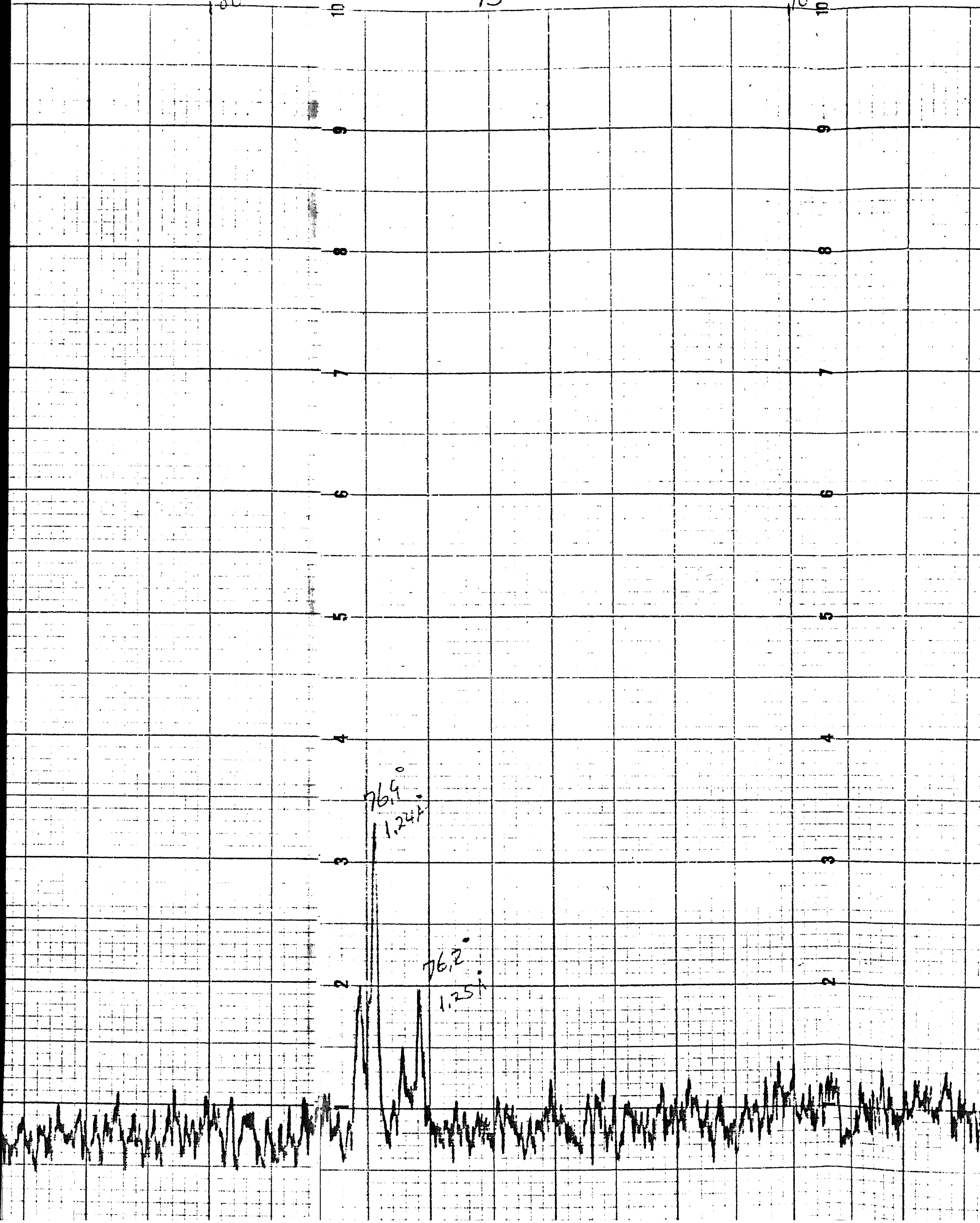

80°
75°
70°
10
9
8
7
6
5
4
3
2
1
76.4°
1.247
76.2°
1.251

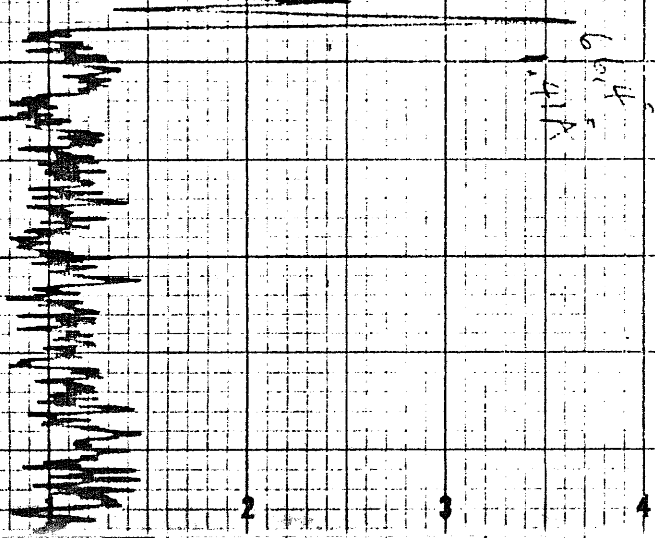

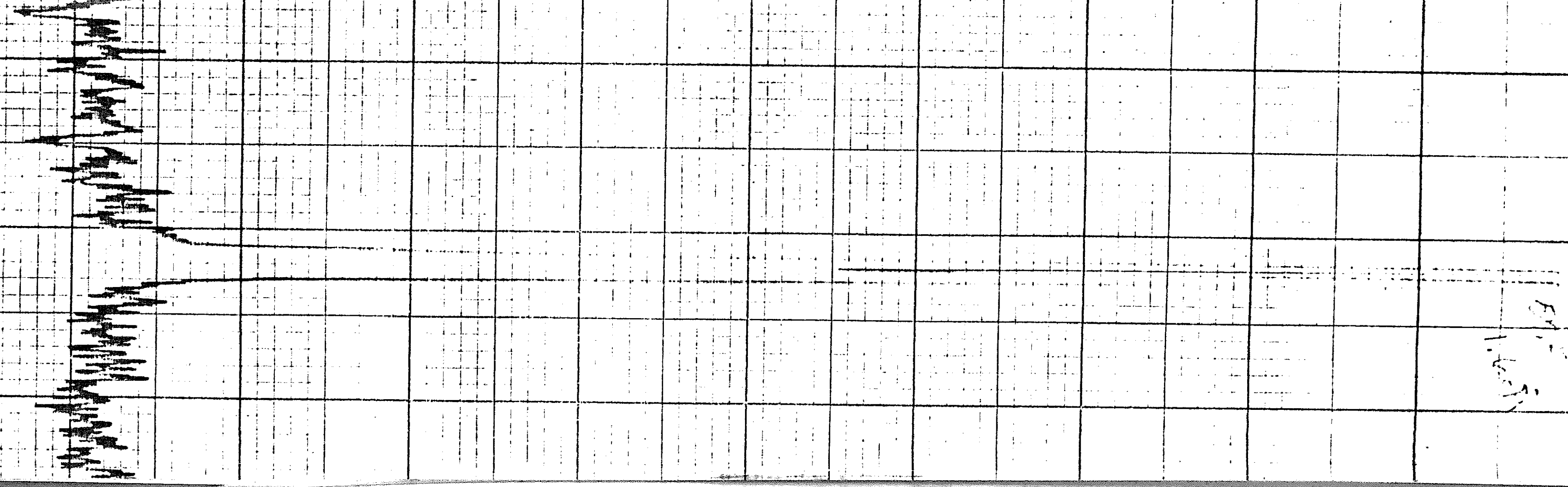

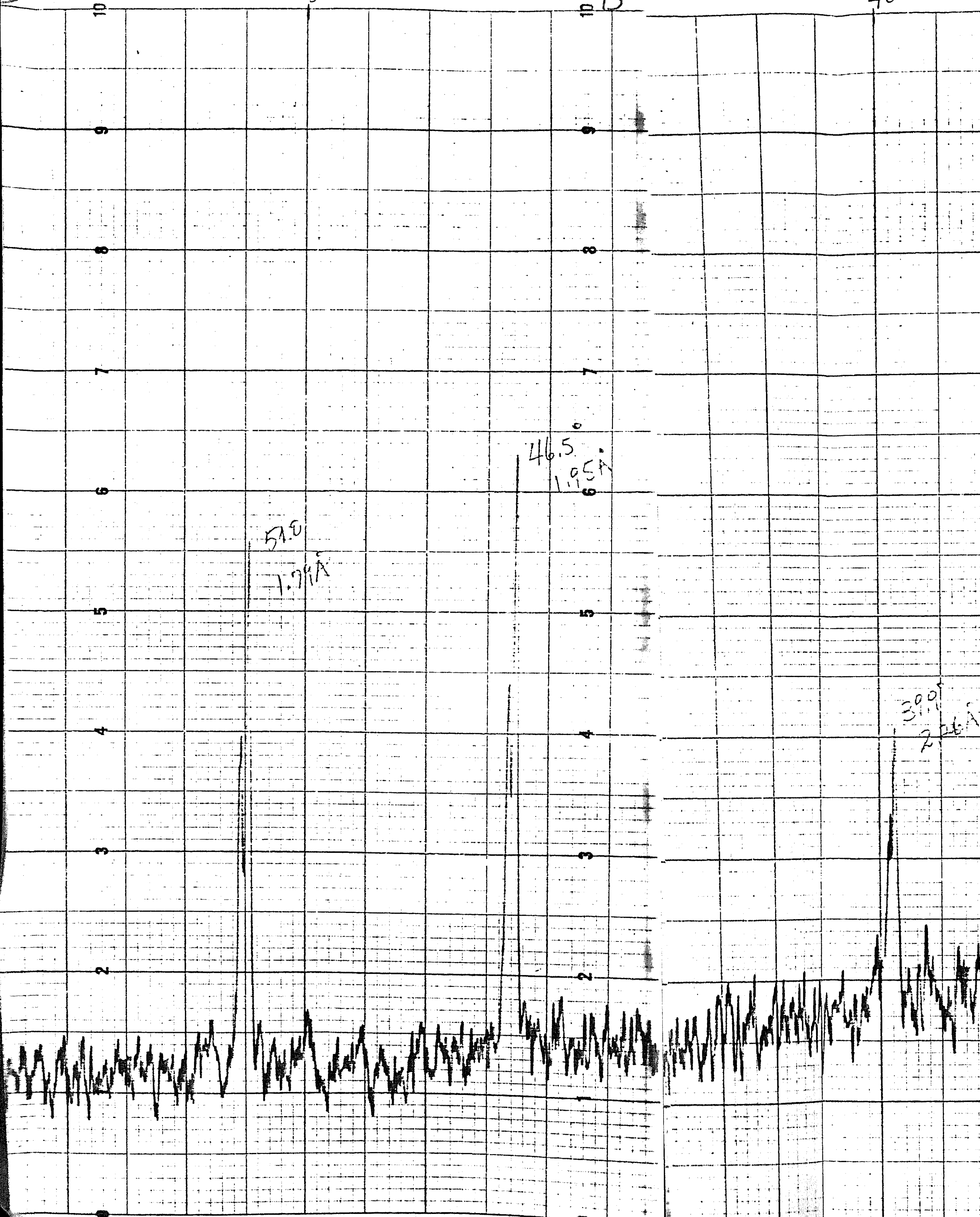

50°
45°
40°
46.5°
1.95Å
51.0
1.79Å

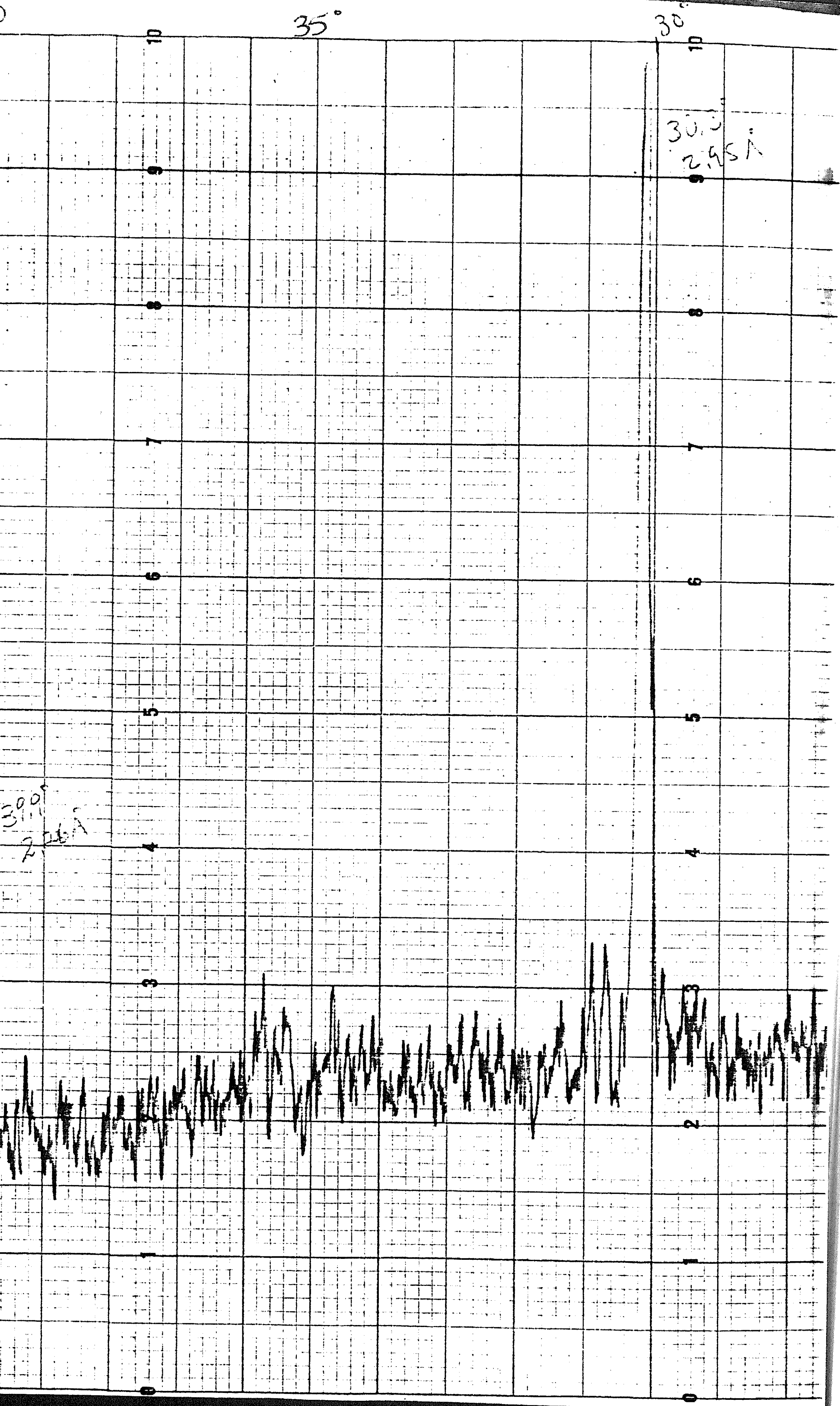

35°
30°
30.0
2.95Å

25° 20° 15°

10
9
8
7
6
5
4
3

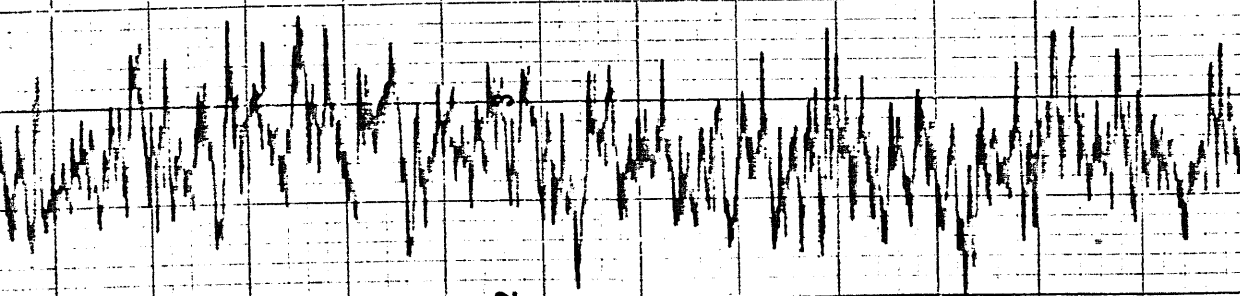

2
1
0

Table 3-1 shows the different interplanar spacing of gallium and the corresponding measured angles of intensity peaks (see figure 3-8). It also compares the theoretical values for gallium intensity peaks given in appendix A with the preceding X-ray diffraction measurement results obtained on the gallium thin films .

NO.	Measured Values		Theoretical Values		Relative	%
	peaks	"d" spacings	peaks	"d" spacings	orientation	Accuracy
1	30.3	2.947 Å	30.23	2.953 Å	111	99.77
2	39.9	2.258 Å	39.82	2.262 Å	020,200	99.80
3	46.5	1.951 Å	46.35	1.957 Å	211	99.68
4	51.0	1.789 Å	51.00	1.789 Å	122	100.0
5	57.5	1.601 Å	57.59	1.599 Å	220	99.84
6	66.4	1.407 Å	66.44	1.406 Å	131	99.94
7	76.2	1.2483 Å	76.26	1.2475 Å	133,313	99.92
8	76.9	1.2387 Å	76.96	1.2379 Å	231	99.93
9	122.	0.8807 Å	118.8	0.8948 Å	326	97.39

Table 3-1 Comparison of gallium intensity peaks

It can be seen from table 3-1 that the gallium thin film, made in the ICBD laboratory, had many different crystal orientations which produced numerous X-ray intensity peaks at various Bragg angles. This sample was found to be polycrystalline and composed of differently oriented small crystallites. It was later discovered that this sample was made by vaccum deposition, which is the evaporation of gallium onto the glass substrate rather than an ion cluster beam deposition as first expected.

In conclusion, it can be observed from the above results and calculations done on the silicon and gallium samples that the X-ray diffractometer and its accessories have a very high degree of accuracy and can be depended on to give reliable results. The oxide layer that grows on the surface of these samples usually does not affect the intensity peak locations but it can however, decrease the amplitude of the intensity peak that is detected by the X-ray diffractometer. To avoid this problem it is recommended that the samples be etched before the X-ray diffraction experiment and should be kept in vacuum, when they are not being used.

After the repair was done on the amplifier section of the X-ray Spectrogoniometer, which was accomplished by replacing a Junction Field Effect Transistor, the X-ray diffractometer has been working properly without much difficulty. Also if the precautions given in appendix C regarding operational procedure and handling are reviewed carefully by a new researcher, he/she should be able to make X-ray diffraction measurements. The two silicon samples with the different orientations along with the ICBD gallium sample can be used as standards to assure proper functioning of the X-ray equipment. Since the gallium X-ray results showed compatibility with the published data, this procedure can be depended on for the measurements that will be done on the gallium nitride samples when they are produced.

APPENDIX A

PROPERTIES OF SILICON AND GALLIUM

1. PROPERTIES OF SILICON

a. Silicon "d" spacings for different orientations [10]

Interplanar spacing "d" (Å)	I/I_1 %	Miller Indices hkl	Bragg angle 2θ
3.1380	100	111	28.4
1.9200	60	220	47.3
1.6380	35	311	56.1
1.3570	8	400	69.2
1.2460	13	331	76.4
1.1083	17	422	88.1
1.0450	9	511	95.0
0.9599	5	440	106.7
0.9178	11	531	114.1
0.8586	9	620	127.6
0.8281	5	533	136.9

Table A-1 Diffraction data for silicon (published data)

I/I_1 is the ratio of the intensity of a peak and the largest peak. (i.e the peak relative to an orientation of 111 has the largest amplitude.) The Bragg angle 2θ is calculated for the Cu $K\alpha_1$ radiation which has a wavelength of $\lambda = 1.5404$ Å.

b. Chemical and molecular properties[11]

Structure .... Diamond Cubic

Lattice constant .... 5.4309 $\mathring{A}$

Closest approach of atoms 2.3517

Atomic number 14

Atomic weight 28.06

Density .... 2.33 g/cm^3 = 0.84 lb/in^3

Atomic volume .... 12.0 cm^3 /g.atom

Melting point .... 1430 ± 20 C or 2605 ± 35 F

Boiling point .... 2300 C or 4200 F

Specific heat .... 0.162 Cal.g/ C

Fusion heat .... 337 Cal/g

2. GALLIUM INTENSITY PEAKS [12]

Interplanar spacing "d" ($\AA$)	Bragg angle 2θ	Miller Indices hkl	I/I_1 %
3.831	23.2	002	28
2.953	30.2	111	100
2.925	30.5	102	50
2.262	39.8	020,200	60
1.996	45.4	113	85
1.957	46.4	211	56
1.947	46.6	022,202	17
1.916	47.4	004	16
1.789	51.0	122	21
1.763	51.8	104	6
1.599	57.6	220	11
1.586	58.1	213	3
1.476	62.9	222	3
1.461	63.6	024,204	14
1.406	66.4	131	9
1.404	66.5	311,302	8
1.391	67.2	124	4

Table A-2 Diffraction data for gallium (published data)

The Bragg angle 2θ is calculated for $\lambda = 1.5404$ $\AA$.

Interplanar spacing "d" (Å)	Bragg angle 2θ	Miller Indices hkl	$I/I_1\%$
1.2766	74.2	006	4
1.2475	76.2	133,313	20
1.2379	77.0	231	14
1.2276	77.7	224	5
1.2216	78.2	215	17
1.1928	80.4	322	15
1.1853	81.1	304	4
1.1302	85.9	040,400	5
1.1119	87.7	026,206	8
1.0866	90.3	411	3
1.0540	93.9	142	1
1.0496	94.4	324	3
1.0355	96.1	117	4
1.0111	99.2	240,420	2
0.9976	101.1	226	2
0.9775	104.0	242,422	1
0.9735	104.6	044,404	5
0.9706	105.0	235	7
0.9626	106.3	217	3
0.9515	108.1	144	1
0.9369	110.6	108	1
0.8986	118.0	431	4
0.8948	118.8	326	2

Table A-2 Diffraction data for gallium (published Data)

The Bragg angle 2θ is calculated for $\lambda = 1.5404$ Å.

APPENDIX B

QUADRATIC FORMS OF MILLER INDICES[13]

	Cubic					Hexagonal	
	hkl						
$h^2+k^2+l^2$	simple	Face-centered	Body-centered	Diamond		h^2+hk+l^2	hk
1	100					1	10
2	110		110			2	
3	111	111		111		3	11
4	200	200	200			4	20
5	210					5	
6	211		211			6	
7						7	21
8	220	220	220	220		8	
9	300,221					9	30
10	310	310				10	
11	311	311	311			11	
12	222	222	222			12	22
13	320					13	31
14	321		321			14	
15						15	
16	400	400	400	400		16	40
17	410,322					17	
18	411,330		411,330			18	
19	331	331		331		19	32

Cubic						Hexagonal	
	hkl						
$h^2+k^2+l^2$	simple	Face-centered	Body-centered	Diamond		h^2+hk+l^2	hk
20	420	420	420			20	
21	421					21	41
22	332		332			22	
23						23	
24	422	422	422	422		24	
25	500,430					25	50
26	510,431		510,431			26	
27	511,333	511,333		511,333		27	33
28						28	42
29	520,432					29	
30	521		521			30	
31						31	51
32	440	440	440	440		32	
33	522,441					33	
34	530,433		530,433			34	
35	531	531		531		35	
36	600,442	600,442	600,442			36	60
37	610					37	43
38	610,532		611,532			38	
39						39	52
40	620	620	620	620		40	
41	621,540,443					41	
42	541		541			42	
43	533	533		533		43	61
44	622	622	622			44	
45	630,542					45	
46	631		631			46	
47						47	
48	444	444	444	444		48	44
49	700,632					49	70,53

Cubic						Hexagonal	
	hkl						
$h^2+k^2+l^2$	simple	Face-centered	Body-centered	Diamond		h^2+hk+l^2	hk
50	710,550,543		710,550,543			50	
51	711,551	711,551		711,551		51	
52	640	640	640			52	62
53	720,641					53	
54	721,633,552		721,633,552			54	
55						55	
56	642	642	642	642		56	
57	722,544					57	71
58	730		730			58	
59	731,533	731,533		731,533		59	

APPENDIX C

X-RAY DIFFRACTOMETER

1. OPERATION

The following is a step by step procedure for the operation of the X-ray diffractometer located in room B5 of the Faculty building of the New Jersey Institute of Technology.

a. Turn on procedure

1) Open the water valve. The water is used to cool the X-ray tube.

2) Turn on the circuit breaker above the water valve.

3) Turn on the power on the X-ray power console by pressing the green (ON) button. The voltage indicator should show a voltage of 45 KVP.

4) After the yellow light comes on, indicating that the left side is ready, press the X-ray (RED) button in. The current indicator should show a current of 30 mA.

5) Remove the X-ray shield from the sample holder and insert the sample in. The sample size is limited by:

a) Thickness : Up to 3/8 in.

b) Width : Up to 1 1/8 in.

c) Length : Up to 3 in.

Place the shield back around the sample holder.

6) Set the main protractor to zero degrees. This is done by disengaging the gears (by turning the grey knob on the far right to "out" position), turning the protractor to zero degrees position and engaging the gears back in by setting the knob to the "in" position.

CAUTION : When turning the main protractor and engaging and disengaging the gears, be gentle and handle with ultimate care since the transmission mechanism can be damaged easily.

7) Set the 700 Detector to the desired settings. The following settings are recommended:

a) Pulse Amplitude (Front counter) : 150-153

b) Amplitude Gain : 4

c) Time Constant : 2.5 sec

d) Range : 2.5 K

e) Pulse Height Selector (PHS) : E

8) Chart recorded settings are recommended to be:

a) Chart switch : OFF

b) Power switch : ON

c) Speed knob : "C"

9) The main protractor settings should be as follows:

a) Right grey knob : IN

b) Left grey knob : HIGH

c) Left metal knob : HIGH

Open the X-ray shutter by moving the red lever across . A red light indicates that the shutter is open and the X-ray tube is operating on the sample. Then set the last knob to:

d) Right metal knob : INCREASE

After the measurements are done and the intensity peaks are observed then follow the turn off procedure.

b. Turn off procedure

1) Close the X-ray shutter.

2) Turn the right metal knob on the main protractor to "OFF" position.

3) Turn off the X-ray machine (RED button).

4) Set the front counter on the 700 Detector slowly back to zero.

5) Turn off the line voltage (GREEN button) .

6) Turn off the circuit breaker.

7) Close the water valve.

2. Suggestions for improvements in X-ray measurements

a. JFET replacement

There is a Junction Field Effect Transistor (JFET) of type NTE132 (New-Tone Electronics in Bloomfield) in the amplifier box that turns with the main protractor and amplifies the diffracted signals to be fed into the 700 Detector. This JFET has been replaced four times and is the source of many of the problems that are related to the X-ray diffractometer. This JFET should be replaced if any of the following symptoms are observed:

a) There is no intensity peak at zero degrees.

b) The chart recorder intensity indicator and its pen are in

the middle or off the bottom of the graph paper.

c) There is movement of the pen even when the X-ray shutter

is closed.

This JFET is located inside the amplifier box. To remove it follow the next few steps:

1) Turn all the X-ray equipment off.

2) Open the two screws that hold the cover of the amplifier and remove the cover.

3) Remove the green printed circuit (PC) board by loosening the plastic screw on top right of the amplifier. Turn the board so that the other board (dark green), that is under it, is exposed.

4) Open the two screws that hold this board and remove it.

5) The JFET is located on the left PC board and is mounted on a white transistor socket. Replace the NTE132 with a new one, making sure that the leads (gate, drain, and source) are in the appropriate socket holes.

6) Do the reverse to put things together.

b. Further recommendations

1) Do not exceed 36 mA when operating at 45 KVP.

2) Do not exceed 1.53 KVDC for the pulse height (front counter).

3) Make sure the front counter is set to zero before the line power is turned on. A high surge current or voltage that is caused by not doing this may exceed the JFET NTE132 factory specifications.

4) Close the X-ray shutter by pressing the silver button on the timer. The timer is a small black box with a time setting dial on it.

5) Do not insert fingers or any part of the body in the X-ray beam.

6) Use the large lead X-ray shield if you plan to be in the room for a long period of time, while the X-ray machine is in use.

APPENDIX D

ETCHING PROCEDURE FOR SILICON SAMPLES

The following steps must be taken before the contacts for the silicon are evaporated onto the samples. The etching procedure removes the oxide layer from the silicon surface for better penetration and adhesion of the material to be evaporated to the silicon wafer's surface. Figure D-1 also shows a summary of the etching steps.

a) Soak the samples in hydroflouric acid (HF) for twenty to thirty minutes.

NOTE: The Hydroflouric Acid must be in a plastic container since this acid dissolves glass.

b) Take the samples out of the HF acid solution and put them in a Methanol solution for 2 to 3 more minutes.

c) Rinse the samples in Trichloroethylene solution.

d) Rinse the samples in Isopropyl Alcohol Solution.

e) Rinse the samples in a new Isopropyl Alcohol solution.

f) Rinse the samples in another Isopropyl Alcohol solution again.

g) Let the samples be in the last container until the evaporator is ready and the samples can be put inside the vacuum chamber immediately.

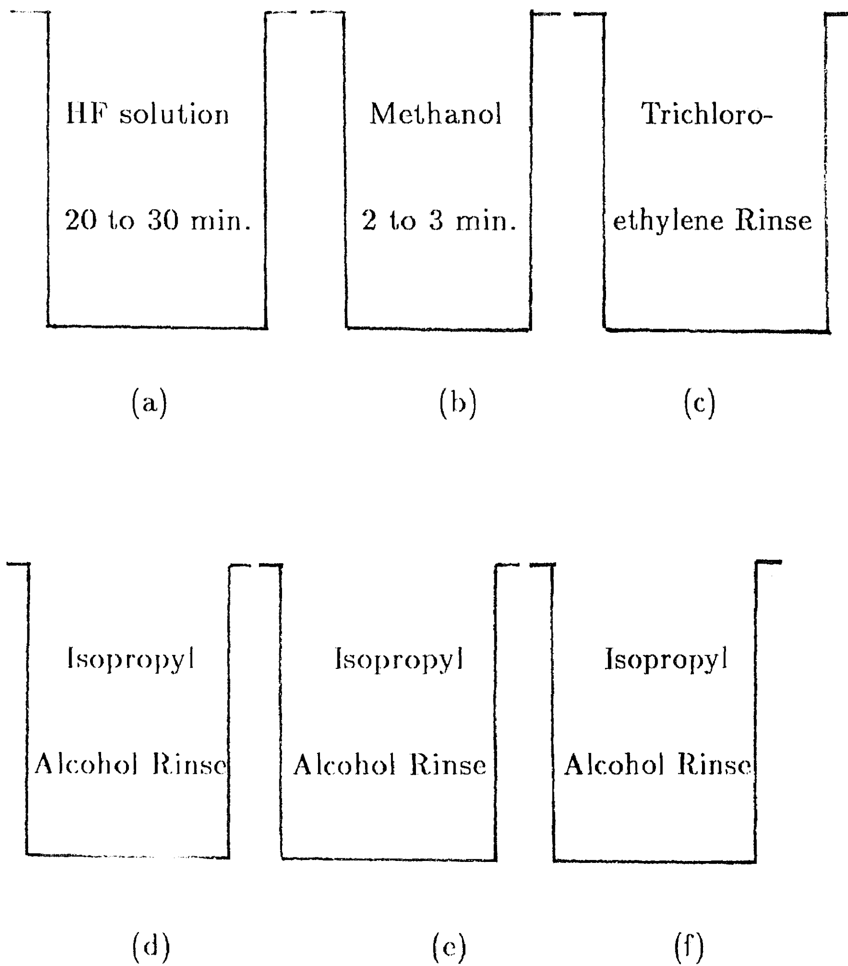

Figure D-1 Etching procedure summary

APPENDIX E

THE JEOL VACUUM EVAPORATOR OPERATION

This is the operational procedure for the Japan Electron-Optics Labratories (JEOL) model JEE4C vacuum evaporator, which is located in room B13 of the Faculty building. This machine is designed to evaporate various metals onto different substrates. A mask is placed on the sample to allow the evaporated metal to cover only the desired portions of the substrate. Figure E-1 shows the basic structure of this equipment.

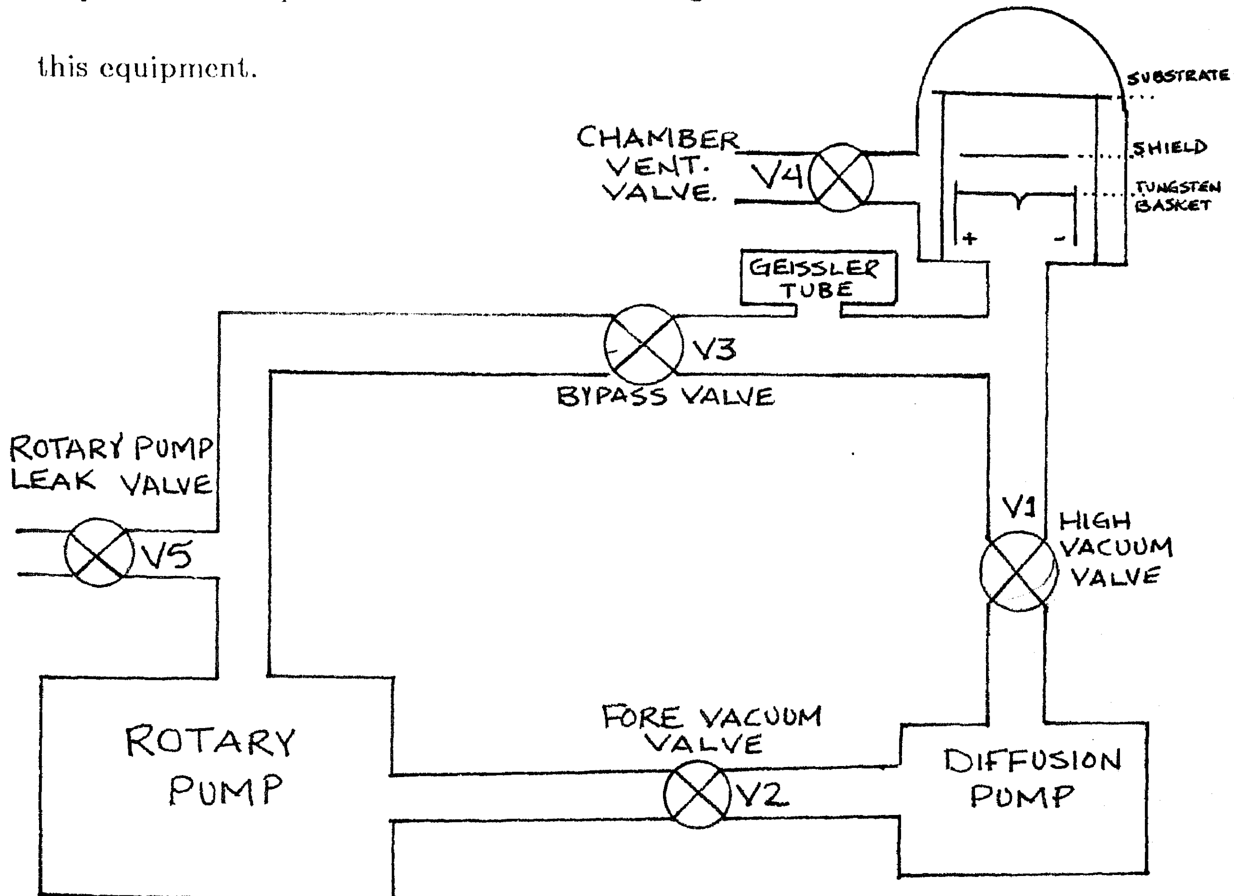

Figure E-1 JEOL vacuum evaporator

Procedure:

1) Turn on all the circuit breakers.

2) Close the rotary pump leak valve (V5).

3) Turn on the main switch on the evaporator.

4) Turn on the rotary pump.

5) After approximately five minutes, open the fore vacuum valve (V2) and wait another five minutes, meanwhile prepare the sample.

6) Set up the sample in the holder and place it in the chamber. After checking the O-ring for damages or cracks, lubricate it and put it in the slot and place the bell jar over the chamber.

> **NOTE: Steps 6 and 7 must be done as quickly as possible to avoid further oxidization of the samples which may result in non-ohmic contacts (approximately 20 to 30 seconds).**

7) Close the chamber ventilation valve (V4).

8) Close the fore vacuum valve (V2) and open the bypass valve (V3) very slowly.

9) After the pressure drops to 0.001 Atm (color of the Geissler tube turns from purple to blue, which takes about 5 to 7 minutes),

10) Close the bypass valve (V3).

11) Open the fore vacuum valve (V2) and then open the high vacuum valve (V1).

12) Turn on the diffusion pump to get high vacuum and lower pressure.

13) Wait until the pressure drops to 10^{-6} Atm. (20 minutes). Check the tube's color. It should be dark. Turn on the heater and apply 15 to 20 mA.

14) After the heater is turned on for about 3 seconds remove the shield.

15) Wait until all the metal is evaporated and the whole tungsten basket glows.

16) Turn down the heater control gradually and turn off the heater.

17) Close the high vacuum valve (V1) and turn off the diffusion pump.

18) After 5 to 10 minutes, which is sufficient time for the diffusion pump to cool down, open the chamber ventilation valve (V4).

19) Let the sample cool off for another 5 minutes.

20) After removing the cover, take the sample out and wait 20 minutes for the rest of the system to cool off.

21) Close the fore vacuum valve (V2).

22) Turn off the rotary pump.

23) Open the rotary pump leak valve (V5).

24) Turn off the main switch.

25) Turn off all the circuit breakers.

Evaporator valves:

V1 : High vacuum valve

V2 : Fore vacuum valve

V3 : Bypass valve

V4 : Chamber ventilation valve

V5 : Rotary pump leak valve

APPENDIX F

PROOF OF THE VAN DER PAUW THEOREM[14]

Let a sample be infinite in all directions. Then apply a current 2i to a point M (see figure F-1):

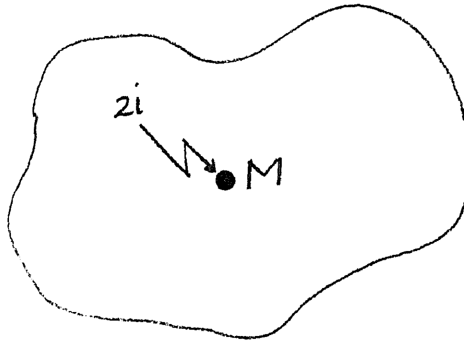

Figure F-1 infinite sample with a point M

This current flows away from M with radial symmetry into infinity. Let d be the thickness of the sample and ρ the resistivity. Then at a distance r from point M the current density is:

$$J = \frac{2i}{2\pi r d} \qquad (F-1)$$

The electric field strength $\mathcal{E}$ is radially oriented and according to the generalized form of Ohm's law:

$$\mathcal{E} = \rho J = \frac{\rho i}{\pi r d} \qquad (F-2)$$

The potential difference between any two point O and P lying on a straight line with M is (see figure F-2)

$$V_p - V_o = \int_p^o \mathcal{E}.dr = \frac{\rho i}{\pi d}\int_o^p \frac{dr}{r} = -\frac{\rho i}{\pi d}\ln(\frac{a+b+c}{a+b}) \qquad (F-3)$$

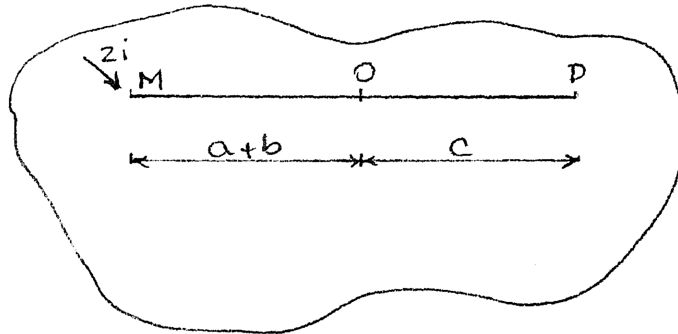

Figure F-2 Current applied to a sample points on a line

No current flows perpendicular to the line MOP. The result is also valid if a part of the sample at one side of this line is omitted yielding a half plane. Also halve the current 2i, cutting it in half (Figure F-3):

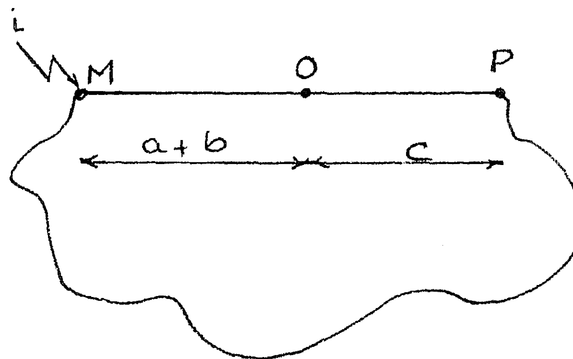

Figure F-3 Semi-infinite sample with half the current applied

Now consider a point N, where a current i flows out from it, which lies on the same line OP. Now we find the resistance (see figure F-4) :

$$R_{MN,OP} = \frac{\rho}{\pi d} \ln \frac{(a+b)(b+c)}{(a+b+c)b} \qquad (F-4)$$

or

$$\frac{(a+b+c)b}{(a+b)(b+c)} = \exp(\frac{-\pi d}{\rho} R_{MN,OP}) \qquad (F-5)$$

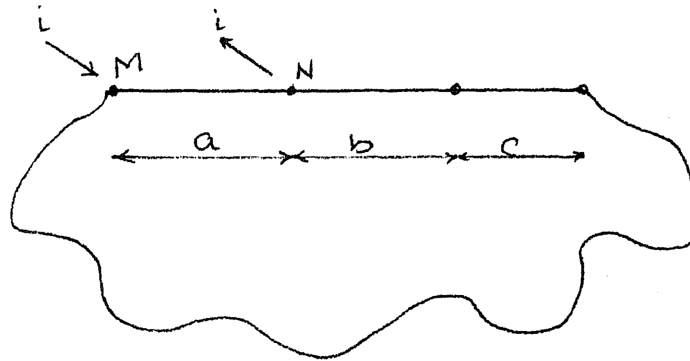

Figure F-4 A sample with four points on a line

Similarly we find:

$$\frac{ac}{(a+b)(b+c)} = \exp(\frac{-\pi d}{\rho} R_{NO,PM}) \qquad (F-6)$$

Addition of the last two equations yields:

$$\exp(\frac{-\pi d}{\rho} R_{NO,PM}) + \exp(\frac{-\pi d}{\rho} R_{MN,OP}) = 1 \qquad (F-7)$$

which is the same as equation (2-11). To derive equation (2-14) which is:

$$\rho = \frac{\pi d(R_{MN,OP} + R_{NO,PM})f}{\ln 2} \qquad (F-8)$$

equation (F-7) is used with:

$$x_1 = \pi d R_{MN,OP} \qquad (F-9a)$$

and

$$x_2 = \pi d R_{NO,PM} \qquad (F-9b)$$

which gives:

$$\exp(\frac{-x_1}{\rho}) + \exp(\frac{-x_2}{\rho}) = 1 \qquad (F-10)$$

then write

$$x_1 = \frac{1}{2}((x_1 + x_2) + (x_1 - x_2)) \qquad (F-11a)$$

and

$$x_2 = \frac{1}{2}((x_1 + x_2) - (x_1 - x_2)) \qquad (F-11b)$$

so equation (F-10) becomes:

$$\exp(-\frac{x_1 + x_2}{2\rho}).(\exp(-\frac{x_1 - x_2}{2\rho}) + \exp(\frac{x_1 - x_2}{2\rho})) = 1 \qquad (F-12)$$

Using the hyperbolic cosine formula:

$$\cosh(x) = \frac{\exp(x) + \exp(-x)}{2} \qquad (F-13)$$

and rewritting equation (F-12) in terms of the hyperbolic cosine function:

$$\exp(-\frac{x_1 + x_2}{2\rho}).\cosh(\frac{x_1 - x_2}{2\rho}) = \frac{1}{2} \qquad (F-14)$$

and letting:

$$(\frac{x_1 + x_2}{2\rho}) = \frac{\ln 2}{f} \qquad (F-15)$$

equation (F-14) becomes:

$$\exp(-\frac{\ln 2}{f}).\cosh(\frac{x_1 x_2 - 1}{x_1 x_2 + 1}.\frac{\ln 2}{f}) = \frac{1}{2} \qquad (F-16)$$

Finally, substituting for x_1 and x_2 from equations (F-9) gives:

$$\rho = \frac{\pi d}{\ln 2}\frac{R_{MN,OP} + R_{NO,PM}}{2} f \qquad (F-17)$$

which is the same as equation (2-14).

"f" is called the correction factor and is a function of the ratio of the two resistances $R_{MN,OP}$ and $R_{NO,PM}$. The graph of f versus the resistance ratio is given in appendix G.

APPENDIX G

HALL EFFECT PROCEDURE

1. Hall effect measurement procedure

This procedure was modified to improve the accuracy of the measurements during this thesis work. The Hall effect set-up is located in room 422 of the Tiernan building. Follow the below procedure after the sample has been tested for true ohmic contacts on a curve tracer.

a. Preparation procedure

1) Open the red water valve for the magnet cooling.

2) Turn on the line power on the Programmable Regatron Power Supply.

3) Gently place the sample on the holder and fasten the probe screws until an adequate contact is reached. This step should be done with ultimate care. When fastening the probe screws press on the ends of the plastic parts so the probes stay off the sample's surface and do not scratch the contacts off. Also do not tighten these screws too tightly because the samples can break easily under moderate pressure.

4) Place the holder into the vacuum chamber and turn on the vacuum pump.

5) Wait until the pressure has dropped to 50 microns of mercury, which can take from 10 to 30 minutes. Meanwhile turn the Keithly 616 Electrometer on and with the range set to volts, automatic sensitivity and normal reading position, zero the dial. This is done by setting the zero check switch and turning the zero dial until a zero reading is obtained.

6) Connect the three wires that are labeled: + , REM + , and REM - from the current control box to the corresponding outlets on the Programmable Regatron Power Supply.

7) Connect the probe wires to the Hall effect control box. Since the holder is two sided select the appropriate side for measurements.

8) Make sure the voltmeter and the current control box are connected to the Hall effect control box and the wire colors match.

9) When a pressure of 50 microns of mercury is reached then proceed with the measurements.

b. Voltage measurements procedure (Constant Magnetic Field)

1) With the Hall effect box switch set to position 2 and normal, turn on the D.C. switch of the Programmable Regatron and tune the current to 1.1 mA. Write the indicated voltage in the appropriate box of the Hall effect data sheet.

CAUTION: Do not leave the D.C. switch of the Programmable Regatron on for more than 4 to 5 seconds for each measurement.

2) Repeat step 1 with the switch set to position 3 and normal.

3) Set the switch to 1 and normal and repeat step 1.

4) Follow step 1 with the switch set to position 1 and reverse.

5) Turn on the magnet and set it to 3500 Gauss (42 A DC)

6) Repeat step 1 with the switch set to position 1 and normal.

7) Set the switch to reverse position (still at 1) and follow step 1.

8) Turn the dial of the magnet 90 degrees clockwise. This reverses the magnetic field.

9) Repeat step 1 with the switch set to 1 and reverse.

10) With the switch set to 1 and normal, repeat step 1.

This concludes one set of measurements for the Hall effect experiments. However, for greater accuracy it is recommended that these sets of measurements be taken eight times.

c. Voltage measurements with variable magnetic field

These sets of measurements correspond to page two of the Hall effect data sheets. All steps taken in section G.1.b. are repeated with the difference that for each set the magnetic field is changed. Therefore for each sample eight more readings are taken for the magnetic fields of : 4620, 4340, 2000, 1000, 765, 432, 250, and 125 Gauss (10^{-8} Wb/cm^2).

d. Recommendations for future measurements

1) Replace the analog ammeter with a digital meter accurate up to 10 μA.

2) Place a 100Ω to 500Ω potentiometer in series with the 500KΩ potentiometer and the 5KΩ potentiometer in the current control box for finer current tuning and control.

3) For each voltage measurements fine tune the current to 1.1 mA.

4) High voltage readings of 1.5 volts or more indicate high resistance or bad ohmic contacts. Check the contacts and probes and repeat the experiment from the start.

5) An off-scale voltage on the Programmable Regatron is an indication of an open circuit. Recheck all the connections for continuity and contact.

6) For the first set of measurements all the values in one column should be within 2 per cent of each other. If however, two readings in a column are more than 5 per cent apart from each other, take that reading again.

7) If a few number of samples are being tested, it is recommended to use the same side of the holder for each measurement for consistency of the result.

2. Hall effect calculation procedure

a. The related equations

There are a set of eight readings taken in the Hall effect measurement. Let these voltage readings be labeled V_2 to V_9 corresponding to columns two to nine of the Hall effect data sheet. The following equations calculate the Hall voltage, resistivity, total impurity concentration, mobility, and the Hall coefficient.

As mentioned in the Van Der Pauw theorem, the Hall Voltage V_H is the difference of the voltages with and without a magnetic field present and normal to the sample. Equation (G-1) utilizes this fact and averages the four differences of :

$$V_H = \frac{|V_6 - V_4| + |V_7 - V_5| + |V_8 - V_5| + |V_9 - V_4|}{4} \qquad (G-1)$$

The resistivity is given by equation (F-16) or (2-15). Rewriting that equation and substituting the new terms we have:

$$\rho = \frac{(V_2 + V_3)}{I} \cdot \frac{\pi d f}{2 \ln 2} \qquad (G-2)$$

where

d - sample thickness (0.0254 cm)

f = correction factor obtained from figure G-1

Figure G-1 on page 81 shows a graph of the correction factor versus the ratio of the two resistances $R_{MN,OP}$ and $R_{NO,PM}$, which in this case is same as the ratio of V_2 and V_3 since the current is always constant at 1.1 mA.

The majority carrier concentration, n_o or p_o, is calculated from equation G-3:

$$n_o(or \quad p_o) = \frac{I_x B_z}{qtV_H} \qquad (G-3)$$

where

I_x = applied current = 1.1 mA,

B_z = Magnetic field in Wb/cm^2,

q = Electron charge = $1.6 \times 10^{-19} V$, and

V_H = Hall voltage in volts.

The mobility is given by equation (G-4):

$$\mu_H = \frac{V_H}{(V_2 + V_3)|B|\frac{\pi f}{2 \ln 2}} \qquad (G-4)$$

and the Hall coefficient is just the product of the mobility and the resistivity.

$$R_H = \mu_H \rho \qquad (G-5)$$

The following section is a program for the HP11-C calculator which facilitates tedious calculations.

b. Hall effect program for the HP11-C calculator

The user must input the following values into the registers (see table G-1):

NO.	VARIABLE	UNITS	REGISTER
1	B	Gauss	1
2	V_2	Volts	2
3	V_3	Volts	3
4	V_4	Volts	4
5	V_5	Volts	5
6	V_6	Volts	6
7	V_7	Volts	7
8	V_8	Volts	8
9	V_9	Volts	9
10	f	None	0

Table G-1 List of inputs and their corresponding registers

After the first nine values are put into to the calculator, the calculator will display the ratio of V_2/V_3 . If this value is smaller than one then take the reciprocal and input the corresponding value of f from graph G-1 to the register 0. The calculator will then calculate and display the values of V_H, μ_H,n_o or p_o, ρ, and R_H respectively.

HALL EFFECT PROGRAM

fLBL A
RCL 2 ENTER RCL 3 ÷ R/S

RCL 6 ENTER RCL 4 - gABS ENTER
RCL 7 ENTER RCL 5 - gABS ENTER
RCL 8 ENTER RCL 5 - gABS ENTER
RCL 9 ENTER TCL 4 - gABS ENTER
4 ÷ STO .0 fPSE fPSE fPSE

RCL 2 ENTER RCL 3 + RCL 1 ×
RCL 0 × RCL .0 ÷ 2.662 EEX 8 - ×
1/X STO .1 fPSE fPSE fPSE

RCL 1 ENTER RCL .0 ÷
270.67 EEX 7 × fPSE fPSE fPSE

RCL 2 ENTER RCL 3 + RCL 0 ×
52.328 × STO .2 fPSE fPSE fPSE

RCL .2 ENTER RCL .1 ×
fPSE fPSE fPSE

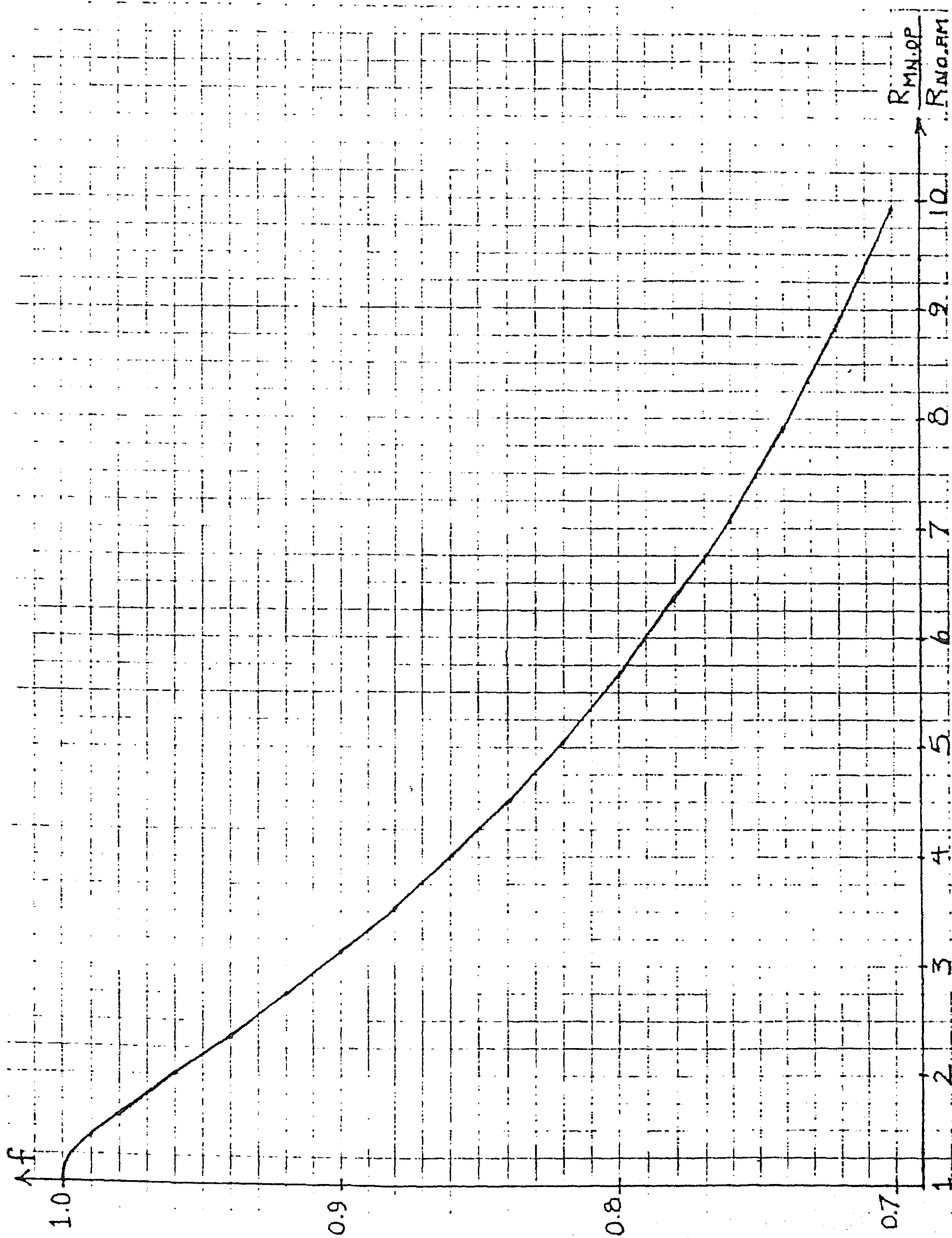

Figure G-1 Van Der Pauw's correction factor "f" vs. $\frac{R_{MN,OP}}{R_{NO,PM}}$

BIBLIOGRAPHY

1 . Streetman, Ben G., Solid State Electronic Devices. 2nd Ed., Englewood Cliffs, NJ:Prentice-Hall, Inc.,1980, pp. 88-90.

2 . Van Der Pauw, L. J., "A Method of Measuring the Resistivity and Hall Coefficient on Lamellas of Arbitrary Shape ," Philips Technical Review, vol. 20, 1958, pp. 220-224.

3 . Muller, Richard S. and Theodore I. Kamins, Device Electronics for Integrated Circuits., New York: John Wiley and Sons, 1976, p. 26.

4 . Muller, Device Electronics for Integrated Circuits, p.27.

5 . Cullity, Bernard Dennis, Elements of X-ray Diffraction., 2nd Ed., Reading , MA : Addison-Wesley Pub. Co., 1978, p. 3.

6 . Cullity, Elements of X-ray Diffraction, p. 277.

7 . Chalmers, Bruce and et. al.,Crystallography, Module 7 : Introduction to X-ray Diffraction, Philadelphia, PA : The Pennsylvania State University Press, 1978.

8 . General Electric Company, The SPG 2 X-ray Spectrogoniometer For Diffraction and Emission Techniques.,X-ray Department of General Electric Company , 1968

9 . Cullity, Elements of X-ray Diffraction, p. 459.

10. Berry, Leonard G., ed. Index to the Powder Diffraction : File 1970 Philadelphia, PA: Joint Committee on Powder Diffraction Standards., p. 1047.

11. Lyman, Taylor, ed., Metals Handbook, 8th Ed., vol. 1, Novelty , Ohio : American Society for Metals, 1961, pp. 1140-1141 .

BIBLIOGRAPHY

12. Berry , Index to the Powder Diffraction : File 1970 , p. 817

13. Cullity, Elements of X-ray Diffraction., pp. 471-472

14. Van Der Pauw, L. J.,"A Method for Measuring specific Resistivity and Hall Coefficient of Discs of Arbitrary Shape," Philips Res. Rpts. Vol. 13, Feb. 1958, p. 13.